Journal of Hazardous Materials 215–216 (2012) 1–16

Contents lists available at SciVerse ScienceDirect

Journal of Hazardous Materials

journal homepage: www.elsevier.com/locate/jhazmat

Review

Application of titanium dioxide in arsenic removal from water: A review

Xiaohong Guan[a,*], Juanshan Du[b], Xiaoguang Meng[c], Yuankui Sun[a], Bo Sun[c], Qinghai Hu[a]

[a] State Key Laboratory of Pollution Control and Resources Reuse, College of Environmental Science and Engineering, Tongji University, Shanghai, PR China
[b] State Key Lab of Urban Water Resource and Environment, Harbin Institute of Technology, Harbin, PR China
[c] Center for Environmental Systems, Stevens Institute of Technology, Hoboken, NJ 07030, USA

ARTICLE INFO

Article history:
Received 6 December 2011
Received in revised form 6 February 2012
Accepted 25 February 2012
Available online 3 March 2012

Keywords:
Adsorption
Photocatalytic oxidation
Nanoparticles
Complexation
Arsenate
Arsenite

ABSTRACT

Natural arsenic pollution is a global phenomenon and various technologies have been developed to remove arsenic from drinking water. The application of TiO_2 and TiO_2-based materials in removing inorganic and organic arsenic was summarized. TiO_2-based arsenic removal methods developed to date have been focused on the photocatalytic oxidation (PCO) of arsenite/organic arsenic to arsenate and adsorption of inorganic and organic arsenic. Many efforts have been taken to improve the performance of TiO_2 by either combing TiO_2 with adsorbents with good adsorption property in one system or developing bifunctional adsorbents with both great photocatalytic ability and high adsorption capacity. Attempts have also been made to immobilize fine TiO_2 particles on supporting materials like chitosan beads or granulate it to facilitate its separation from water. Among the anions commonly exist in groundwater, humic acid and bicarbonate have significant influence on TiO_2 photocatalyzed oxidation of As(III)/organic arsenic while phosphate, silicate, fluoride, and humic acid affect arsenic adsorption by TiO_2-based materials. There has been a controversy over the TiO_2 PCO mechanisms of arsenite for the past 10 years but the adsorption mechanisms of inorganic and organic arsenic onto TiO_2-based materials are relatively well established. Future needs in TiO_2-based arsenic removal technology are proposed.

Contents

* Corresponding author. Tel.: +86 21 65980956.
E-mail addresses: guanxh@tongji.edu.cn (X. Guan), dujuanshan1209@yahoo.com.cn (J. Du), xmeng@stevens.edu (X. Meng), yksun03@163.com (Y. Sun), sunbo880628@163.com (B. Sun), huqinghaihqh@163.com (Q. Hu).

0304-3894/$ – see front matter © 2012 Elsevier B.V. All rights reserved.
doi:10.1016/j.jhazmat.2012.02.069

1. Introduction

During the past two decennia arsenic poisoning via groundwater has become a worldwide problem. Arsenic contaminated groundwater has been found in aquifers in Bangladesh, China, India, Nepal, Argentina, Mexico, Taiwan, etc. [1,2]. Elevated levels of arsenic groundwater not only cause significant problems in the provision of safe drinking water [3], but lately have also raised concern regarding food safety [4,5]. Long-term exposure to arsenic has been associated with cancer of the skin, lungs, urinary tract, kidneys and liver, and can also produce various other non-cancerous effects [6]. Therefore, the World Health Organization (WHO) has reduced the guideline for arsenic in drinking water from 50 to 10 $\mu g\,L^{-1}$ and most industrialized countries also take 10 $\mu g\,L^{-1}$ as a statutory limit.

Inorganic and organic arsenic occur naturally in the environment, with inorganic forms being most abundant [2]. Weathering of rock is the major natural source of inorganic arsenic, and it is also released by human activities. Inorganic arsenic in groundwater is present mainly in nonionic trivalent (As(III)) and ionic pentavalent (As(V)) forms in different proportions depending on the environmental conditions of the aquifer [7]. The speciation of arsenic in water is usually controlled by redox conditions, pH, biological activity, and adsorption reactions [7,8]. The reducing condition at low Eh value converts arsenic into As(III) form, whereas at high Eh value As(V) is the major arsenic species. As(III) is more toxic than As(V) and difficult to remove from water by most techniques [9]. Thus, As(III) is typically removed by first oxidizing it to As(V) and then As(V) is removed using adsorption, precipitation, or ion exchange processes [10]. Organic arsenic species, notably monomethylarsonic acid (MMA) and dimethylarsinic acid (DMA), are introduced into the environment primarily through agricultural and industrial activities [11]. MMA and DMA are active ingredients in products commonly used for weed control and defoliation prior to cotton harvesting, and occur as problematic pollutants in groundwater at sites with a history of pesticide manufacturing and improper disposal [12]. While methylation of inorganic arsenic has been proposed as a biological detoxification process, recent research indicates that methylated arsenic species cause DNA damage, chromosomal aberrations, and tumor promotion in mice and rats [13,14]. Despite the fact that inorganic species are predominant in natural waters, the presence of MMA and DMA has also been reported [12,15].

Various technologies have been adopted to remove inorganic species of arsenic from drinking water, but only few methods have been developed to remove organic arsenic species [11]. Existing arsenic removal technologies reported in the literature may be lumped in the following main categories: oxidation, precipitation, coagulation, membrane separation, ion exchange, biological treatment and removal systems, chemisorption filtration, and adsorption [10,16–20]. Most of the established technologies for arsenic removal make use of several of these processes, either at the same time or in sequence. Mohan and Pittman Jr. [21] compared the commonly used arsenic removal technologies and concluded that all methods suffer from one or more drawbacks, limitations and scope of application. Adsorption is one of the most commonly used methods for either inorganic or organic arsenic removal from drinking water. Arsenic sorption by commercially available activated carbons and other low-cost adsorbents are surveyed and critically reviewed and their sorption efficiencies were compared in a recent review [21]. Mohan and Pittman Jr. [21] offered a valuable review and summarized commercially available carbons. In the adsorption-based arsenic removal methods, many studies utilize activated alumina [22–24] and various iron oxides/hydroxides [25–27] as the adsorption media.

As illustrated in Fig. 1, at the near-neutral pH typical of most groundwaters [1], As(III) exists as neutral species (H_3AsO_3), whereas As(V) exists as anionic species ($H_2AsO_4^-$ or $HAsO_4^{2-}$). Thus most methods used for arsenic removal exhibit higher affinity for As(V) compared to As(III). With regard to MMA and DMA, the molecular size is larger than As(V) and has less coordination sites in one molecule although they are ionic species in most natural waters, as shown in Fig. 1. Removal of MMA and DMA by many adsorbents, e.g., manganese greensand, iron oxide coated sand and TiO_2 was not efficient [11,28]. Thus the preoxidation process for converting As(III)/organic arsenic to As(V) is essential to exploit the full potential of arsenic removal system [15,29]. TiO_2 is a promising material for arsenic removal from water due to its physical and chemical stability, negligible toxicity, the resistance to corrosion [30] as well as strong oxidizing power of the holes, redox selectivity, high photo-stability, easy preparation and high affinity to arsenic [31]. Photocatalysis with TiO_2 offers a relatively inexpensive, environmentally benign way to achieve As(III) oxidation [32,33]. Moreover, TiO_2 can work as adsorbent to remove As(V) from water [9,34,35]. The bi-functional property of TiO_2 gives it an additional advantage and many studies have been carried out to investigate arsenic removal by TiO_2. However, up to now a comprehensive review on the application of TiO_2 in arsenic removal is lacking. Therefore, the objectives of this study were to summarize (1) the performance of TiO_2-catalyzed photocatalytic oxidation (PCO) of As(III)/organic arsenic and arsenic adsorption by various TiO_2; (2) the methods to improve arsenic removal by TiO_2; (3) the influence of co-existing solutes on arsenic removal by TiO_2; (4) the mechanisms of As(III)/organic arsenic oxidation by TiO_2-catalyzed photocatalytic reaction and arsenic adsorption on TiO_2.

2. Arsenic removal by various TiO_2

The application of TiO_2 in arsenic removal can be divided into two aspects: TiO_2 functions as both photocatalyst and adsorbent in the presence of UV light or sunlight irradiation but it works only as adsorbent in the absence of irradiation, as illustrated in Fig. 2. Thus, the application of TiO_2 in PCO of As(III)/organic arsenic and in adsorption of various arsenic species will be reviewed separately in this part.

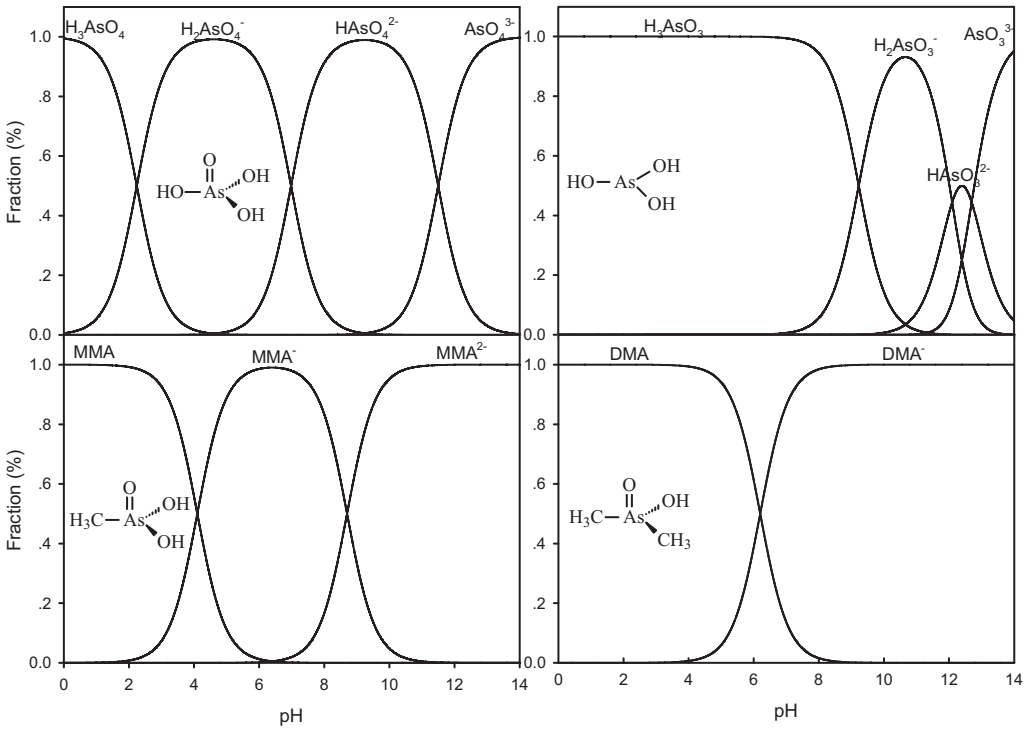

Fig. 1. Species distribution of various arsenic as a function of pH (The pK_a values of various arsenic were adopted from [11]).

2.1. TiO_2-catalyzed photooxidation of As(III) and organic arsenic

TiO_2 photocatalytic oxidation is a promising technology for converting As(III)/organic arsenic to As(V) and has been reported by a number of groups [36–42]. Yang et al. [36] demonstrated for the first time that in the presence of UV light, TiO_2 (2 g L^{-1}) and an electron scavenger (O_2 in this case), the oxidation of As(III) (525 μM) to As(V) was reasonably facile and was complete within 30 min at pH 9. Bissen et al. [41] investigated the TiO_2-catalyzed photooxidation of As(III) to As(V) in aqueous TiO_2 suspensions using a solar simulator which emitted ultraviolet and visible radiations. The concentration of As(III) was varied between 50 μg L^{-1} and 10 mg L^{-1}, and the concentration of TiO_2 between 1 and 50 mg L^{-1}. Complete oxidation of As(III) to As(V) occurred within minutes and the concentration of As(III) declined exponentially which indicated first-order kinetics. In the pH range between 5 and 9 there was no significant influence of the pH of the suspension on the reaction rate. As(III) was also oxidized by UV radiation in the absence of TiO_2, but the reaction was slower than in the presence of TiO_2 resulting in an irradiation time too long for practical use. In addition, oxidation of As(III) in the presence of TiO_2 was also observed under solar irradiation within a few minutes. Xu et al. [42] also observed an extremely high As(III) oxidation rate in the TiO_2 photocatalysis process. They determined As(III) PCO under the conditions of air saturation and TiO_2 concentration of 1 g L^{-1} and found that the adsorption of As(III) onto the surface of the TiO_2 prior to irradiation was greater than 97% under their experimental conditions. The oxidation of As(III) was extremely fast, and within 1 min of irradiation of the TiO_2 suspension over 90% of the As(III) had been converted to As(V).

Lee and Choi [37] reported that As(III) oxidation in UV-illuminated TiO_2 suspension was highly efficient in the presence of dissolved oxygen and the initial PCO rate of As(III) was faster at pH 9 than at pH 3. In both cases, the oxidation was completed within 2 h of irradiation. Both humic acid and ferric ions were beneficial to the PCO of As(III). Ryu and Choi [39] further showed that surface modification through the deposition of noble metals such as Pt on TiO_2 particles significantly enhanced the PCO of As(III) by trapping conduction band (CB) electrons and consequently retarding the fast charge-pair recombination.

Jayaweera et al. [38] also reported that in the presence of 0.25 g L^{-1} TiO_2 photocatalyst and UV radiation (250 W, <300 nm), nonionic H_3AsO_3 (100 mg L^{-1}) can be readily oxidized to the anionic form of As(V) with no formation of metallic arsenic. They also observed that pH had little influence on the rate of PCO of As(III) but bubbling air during irradiation showed enhanced rate for As(III) depletion.

Dutta et al. [40] demonstrated that PCO of As(III) to As(V) took place in minutes and followed zero order kinetics. The zero-order rate constant, k, was determined to be 3.47 μM min^{-1}. The study by Bissen et al. [41] showed first-order kinetics at different initial As(III) concentrations and TiO_2 loadings when experimental measurements were made at wavelengths below 260 nm, a region where As(III) absorbs. The kinetic measurements in their

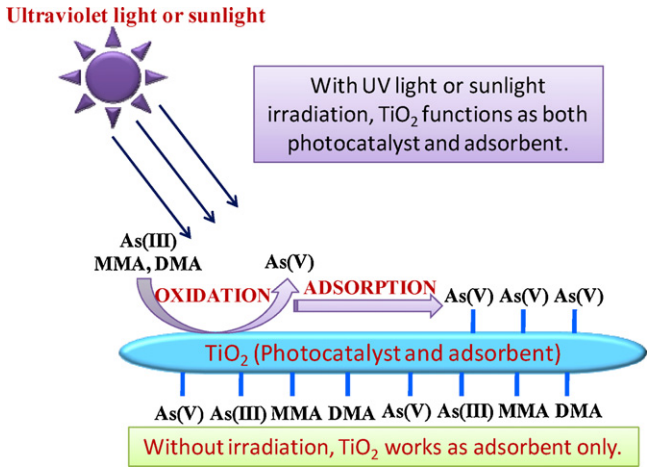

Fig. 2. Schematic illustration of TiO_2 application in arsenic removal.

experiments thus represent a combination of photolysis and PCO of As(III). On the other hand, the light source employed by Dutta et al. [40] had an irradiation spectrum at wavelengths greater than 313 nm with a sharp peak at 365 nm, which may result in different kinetic behavior. This was supported by zero order kinetics behavior observed by Bissen et al. [41] for As(III) oxidation in TiO_2 suspensions under solar irradiation. Dutta et al. [40] also found that the overall As(III) oxidation rate increased with an increase in the catalyst loading or light intensity. The oxidation of As(III) was completed in less than 15 min at all pH values and pH had no influence on As(III) oxidation, consistent with the phenomenon noticed by Jayaweera et al. [38]. The large difference in As(III) oxidation rate in this study and the work of Lee and Choi [37] maybe due to reactor design (i.e., specifically mixing and the contact area with the solid), initial As(III) concentration, and the amount of TiO_2 used in two studies.

Ferguson et al. [33] performed tests for PCO of As(III) in batch systems at pH 6.3 with 0.8–42 μM As(III) and 0.05 g L^{-1} TiO_2. Complete oxidation of As(III) was observed within 10–60 min of irradiation at 365 nm, depending on the initial As(III) concentration. As the total concentration of As(III) dosed to the TiO_2 suspension increased from 0.83 to 42 μM (the suspension was stirred in the dark for 30 min to allow the system to attain sorption equilibrium), the kinetics of TiO_2-photocatalyzed As(III) oxidation with respect to dissolved As(III) shifted from pseudo first-order kinetics toward pseudo zero-order kinetics, which was consistent with surface saturation at higher concentrations. Ferguson and Hering [32] also designed a flow-through, fixed-bed reactor with glass beads, which were coated with mixed P25/sol–gel TiO_2, inside and the reactor was open on top so the system could be irradiated from above. The influences of the reactor residence time, influent As(III) concentration, number of TiO_2 coatings on the beads, solution matrix, and light source on As(III) oxidation were determined. This system achieved efficient oxidation of As(III) to As(V) under both UV irradiation and natural sunlight. Inhibition of the photocatalyst activity either by the product As(V) or by the competing adsorbates phosphate and fluoride was not observed, suggesting that practical application may be feasible without frequent photocatalyst regeneration. The fixed-bed TiO_2 reactor offered an environmentally benign method for As(III) oxidation. Tsimas et al. [43] also reported that the rate of PCO of As(III) was dependent on As(III) concentration. They investigated the PCO of As(III) at 50 mg L^{-1} TiO_2 loading, pH 6.4 and noted that complete As(III) oxidation could be accomplished in 10, 15, 30 and 30 min when the initial As(III) concentrations were 3, 5, 10, 20 mg L^{-1}, respectively.

Xu and Meng [44] investigated the physicochemical properties of TiO_2 particles in the diameter range between 6.6 and 30.1 nm and the effect of the crystalline size on a photocatalytical oxidation. Their results revealed that there was not much difference in the rate of As(III) photooxidation when the diameter of the TiO_2 nanoparticles was between 6.6 and 14.8 nm. However, the As(III) photooxidation rate clearly decreased when the particle size increased to 30.1 nm. Although TiO_2 with a larger surface area should have a faster oxidation rate [45], the band gap of ultrafine semiconductor particles increases with decreasing particle size when it is smaller than the band gap minimum [44]. Thus the combined effect of band gap change and the specific surface area (or particle size) of the TiO_2 photocatalysts determined the photocatalytic reactivity of TiO_2 [46]. This could explain why the photooxidation rate constants (k) of As(III) by TiO_2 with a size less than 14.8 nm were equal.

The efficiency of PCO of As(III) and the conditions under which the experiments were carried out were summarized in Table 1 for comparison. The oxidation rates and efficiency of the photocatalytic system are highly dependent on a number of the operation parameters, e.g., TiO_2 loading, properties of TiO_2, pH, temperature, dissolved oxygen, light wavelength, light intensity, as well as photocatalytic reactor configuration [47]. Moreover, the co-existing solutes also affect the PCO of As(III) and organic arsenic, which will be discussed in Section 4.1. Thus, it is extremely difficult to compare these results as the experimental conditions varied a lot between different research groups. Anyway, Table 1 reveals that As(III) can be effectively oxidized to As(V) in TiO_2-catalyzed photooxidation process under environmental relevant conditions.

Xu et al. [11] reported that the PCO of MMA and DMA was highly efficient in the air-saturated suspensions. DMA could be oxidized to MMA as the primary oxidation product, which was subsequently oxidized to inorganic As(V). The degradation of MMA and DMA under TiO_2 PCO occurred with half-lives of approximately 4 and 7 min for MMA and DMA at pH ~ 6.8, respectively. The PCO of organic arsenic was pH dependent and the fastest degradation of MMA was observed at pH 3 and 7, while the degradation of DMA was fastest at pH 3, and slightly slower at pH 7. Both MMA and DMA were degraded relatively slowly at pH 10. These trends were consistent with the pH effect of the adsorption. The mineralization of MMA and DMA by TiO_2 photocatalysis followed the Langmuir–Hinshelwood kinetic model.

Xu et al. [15] revealed that in the presence of UV irradiation and 0.02 g L^{-1} TiO_2, 93% MMA (initial concentration is 10 mg-As L^{-1}) was transformed into inorganic As(V) after 72 h of a batch reaction. The mineralization of DMA to As(V) occurred in two steps with MMA as an intermediate product. The photodegradation rate of MMA and DMA could be described using first-order kinetics, where the apparent rate constants were 0.033 and 0.013 h^{-1} for MMA and DMA, respectively.

Phenylated arsenic compounds including 4-hydroxy-3-nitrophenylarsenic acid (roxarsone), 4-aminophenylarsenic acid (p-arsanilic acid), etc. are commonly utilized in the broiler poultry industry as feed additives to control cecalcoccidiosis [48] have become a serious environmental concern [49]. Zheng et al. [49] demonstrated that phenylarsonic acid (PA) was readily degraded by TiO_2 photocatalysis. The pH of the solution influenced the adsorption and photocatalytic degradation of PA due to the surface charge of TiO_2 photocatalyst and speciation of PA. The apparent rate constant (k_r) of the TiO_2 photocatalysis of PA at the initial stage was 2.8 μmol L^{-1} min^{-1} and the pseudo-equilibrium constant (K) for PA was 34 L $mmol^{-1}$. TiO_2 photocatalysis resulted in the rapid destruction of PA and may be attractive for the remediation of a variety of organoarsenic compounds.

2.2. Arsenic adsorption on various TiO_2

Many studies have been carried out to investigate the adsorption of inorganic arsenic and organic arsenic on TiO_2 of different properties. The TiO_2 employed in the literatures can be divided into several categories: nanocrystalline TiO_2 particles, titanate nanotubes, hydrous TiO_2, granular TiO_2 and TiO_2-impregnated chitosan beads. The adsorption behavior of arsenic on each TiO_2 category was reviewed in this part.

2.2.1. Nanocrystalline TiO_2 particles

Dutta et al. [34] examined arsenic adsorption on two commercially available nanocrystalline TiO_2 suspensions, Hombikat UV100 (average primary particle < 10 nm) and Degussa P25 (average primary particle ~30 nm) as functions of pH and initial arsenic concentration. Both As(V) and As(III) adsorbed more onto Hombikat UV100 particles than Degussa P25 particles, which should be ascribed to the much higher specific surface area of Hombikat UV100 particles (334 m^2 g^{-1}) than that of Degussa P25 particles (55 m^2 g^{-1}). Adsorption of As(V) onto TiO_2 suspensions was more than As(III) at pH 4 while the adsorption capacity of As(III) was

Table 1
Efficiency of TiO_2-catalyzed photooxidation of As(III) under air equilibrium condition.

$[As(III)]_0$ (mg As L^{-1})	Catalyst	Concentration of catalyst (g L^{-1})	pH	Light source	Light flux	Time (min)	Percentage of oxidation	Ref.
39.375	TiO_2 (Degussa P25)	2	9	A 400 W medium pressure mercury arc lamp	1.83×10^{-5} Einstein min^{-1}	30	~100%	[36]
0.1	TiO_2 (Degussa P25)	0.01	5–9	A 1000-W Xe short-arc lamp, $\lambda < 320$ nm	3×10^{-5} Einstein m^{-2} s^{-1}	3.3	>98%	[41]
3.75	TiO_2 (Degussa P25)	1.5	3 or 9	A 300-W Xe arc lamp (Oriel), $\lambda > 300$ nm	N.A.	120	~100%	[37]
100	TiO_2 from BDH chemicals	0.25	7	A 250 W medium pressure mercury arc discharge lamp, $\lambda > 300$ nm	N.A.	60–90	80%	[38]
37.5	TiO_2 (Degussa P25)	0.5	3	A 300-W Xe arc lamp (Oriel), $\lambda > 300$ nm	N.A.	180	>90%	[39]
37.5	TiO_2 (Degussa P25)	0.5	9	A 300-W Xe arc lamp (Oriel), $\lambda > 300$ nm	N.A.	180	~77%	[39]
37.5	Pt-TiO_2	0.5	3 or 9	A 300-W Xe arc lamp (Oriel), $\lambda > 300$ nm	N.A.	180	~100%	[39]
1.0	TiO_2 (Degussa P25)	1	NA	16 phosphor-coated low-pressure mercury lamps, $\lambda = 350$ nm	$1.5–5 \times 10^{16}$ (proton/s)/cm^3)	7	~100%	[42]
7.5	TiO_2 (Degussa P25)	0.01	3	A 4-W UV lamp (Sankyo Denki, Japan, F4T5BL ($\lambda_{max} = 352$ nm))	1.56×10^{-6} Einstein L^{-1} s^{-1}	30	~40%	[87]
3.0	TiO_2 (Degussa P25)	0.1	9	Philips HPR 125 W high-pressure mercury vapor, $\lambda_{max} = 365$ nm	12.5 mW/cm^2	~12.5	~100%	[40]
0.062	TiO_2 (Degussa P25)	0.05	6.3	A 8 W, 365 nm lamp (UVP model UVL-28)	7.8×10^{16} photons s^{-1}	10	~100%	[33]
0.188	TiO_2 (Degussa P25)	0.05	6.3	A 8 W, 365 nm lamp (UVP model UVL-28)	7.8×10^{16} photons s^{-1}	15	~100%	[33]
0.622	TiO_2 (Degussa P25)	0.05	6.3	A 8 W, 365 nm lamp (UVP model UVL-28)	7.8×10^{16} photons s^{-1}	60	~100%	[33]
5.63	TiO_2 (Degussa P25)	0.1	3	A 4-W UV-A lamp (Sankyodenki, F4T5BLB, $300 < \lambda < 400$ nm)	N.A.	40	~80%	[91]
3.0	TiO_2 (Degussa P25)	0.05	6.4	9 W lamp (Radium Ralutec, 9 W/78), $350 < \lambda < 400$ nm	4.69×10^{-6} Einstein min^{-1}	10	~100%	[43]
5.0	TiO_2 (Degussa P25)	0.05	6.4	9 W lamp (Radium Ralutec, 9 W/78), $350 < \lambda < 400$ nm	4.69×10^{-6} Einstein min^{-1}	10	~100%	[43]
10.0	TiO_2 (Degussa P25)	0.05	6.4	9 W lamp (Radium Ralutec, 9 W/78), $350 < \lambda < 400$ nm	4.69×10^{-6} Einstein min^{-1}	30	~100%	[43]
20.0	TiO_2 (Degussa P25)	0.05	6.4	9 W lamp (Radium Ralutec, 9 W/78), $350 < \lambda < 400$ nm	4.69×10^{-6} Einstein min^{-1}	30	~100%	[43]
15.0	TiO_2 (Degussa P25)	0.5	3	A 300-W Xe arc lamp (Oriel), $\lambda > 300$ nm	$3.46(\pm 0.26) \times 10^{-3}$ Einstein L^{-1} min^{-1}	180	~100%	[29]

N.A.: not available.

more at pH 9, which should be associated with the variation of TiO_2 surface charge and arsenic species with pH.

Ferguson et al. [33] determined the adsorption (in the dark) of both As(III) and As(V) on Degussa P25 TiO_2 at pH 6.3 over a range on dissolved arsenic concentrations, $[As]_{diss}$ of 0.10–89 μM and 0.2 or 0.05 g L^{-1} TiO_2 for As(III) and As(V), respectively. They found that adsorption isotherms generally followed the Langmuir–Hinshelwood model with As(III) exhibiting an adsorption maxima of 32 μmol g^{-1}. As(V) adsorption did not reach a plateau under the experimental conditions examined; the maximum amount of adsorption was 130 μmol g^{-1}.

Pena et al. [9] evaluated the effectiveness of nanocrystalline TiO_2 (primary crystalline size: 6 nm) for As(V) and As(III) adsorption. The removal of As(V) and As(III) reached equilibrium within 4 h and the adsorption kinetics could be described by a pseudo-second-order equation. TiO_2 was effective for As(V) removal at pH < 8 and showed a maximum removal for As(III) at pH of ~7.5 in the challenge water. The adsorption capacity of the TiO_2 for As(V) and As(III) was much higher than fumed TiO_2 (Degussa P25) and granular ferric oxide. More than 0.5 mmol g^{-1} of As(V) and As(III) was adsorbed by the TiO_2 at an equilibrium arsenic concentration of 0.6 mM. The authors concluded that the nanocrystalline TiO_2 was an effective adsorbent for As(V) and As(III).

As(V) removal by commercial P25 nanoparticles produced by Degussa (Germany) was investigated by Jézéquel and Chu [35]. Kinetic results revealed that As(V) adsorption was almost instantaneous and apparent equilibrium was achieved in less than 5 min. The extent of As(V) adsorption decreased with increasing pH in a linear fashion owing to the decrease of positively charged binding sites on the TiO_2 surface. The maximum uptake capacity ranged from 8 mg g^{-1} at pH 3 to 2.7 mg g^{-1} at pH 7.

Xu et al. [11] reported that the adsorption capacities of Degussa P25 TiO_2 under dark conditions at pH ~6.8 for As(V), As(III), MMA and DMA were 11.9, 12.9, 6.5 and 2.8 mg g^{-1}, respectively. The presence of the two methyl groups and only one hydroxyl group on DMA compared to MMA with one methyl group and two hydroxyl groups has direct influence on the adsorption behavior. The adsorption capacity ratio of DMA:MMA:As(V) was approximately 1:2:3, which paralleled the ratio of hydroxyl groups (chelating groups) in the three arsenic species. Therefore, the oxidation of organic arsenic to increase the hydroxyl groups in arsenic molecular could facilitate its removal via TiO_2 adsorption. The authors also found that pH had a strong influence on DMA and MMA adsorption by TiO_2, which may be associated with the distribution of arsenic species and the variation of TiO_2 surface charge with pH.

Xu and Meng [44] synthesized TiO_2 particles with diameter ranging from 6.6 to 30.1 nm by calcining nanocrystalline TiO_2 at different temperatures and evaluated the effect of the crystalline size on arsenic adsorption. TiO_2 prepared at higher temperature had larger particle size and smaller specific surface area. The adsorption capacity of TiO_2 for As(III) and As(V) increased linearly with increasing specific surface area of the particles. The maximum arsenic adsorption capacity of 6.6 nm TiO_2 for As(V) was calculated by the Langmuir model to be 30.5 mg g^{-1}, while for the TiO_2 calcined at 200, 350, 500 and 700 °C, it decreased to 28, 18, 9.86 and 3.62 mg g^{-1}, respectively. The adsorption capacities of the TiO_2 for As(III) were slightly less than that for As(V).

Jegadeesan et al. [51] prepared amorphous TiO_2 nanoparticles (S-TiO_2) and crystalline TiO_2 nanoparticles by calcining the amorphous TiO_2 nanoparticles at different temperatures (designated A-, B-, C-, D-TiO_2, respectively). They also purchased commercially available crystalline TiO_2 (designated H-TiO_2, Hydroglobe Inc., NJ) prepared via sol–gel synthesis of titanium sulfate salts for comparison purpose. The authors [51] investigated the size and crystallinity effects on arsenic sorption capacities and possible As(III) oxidation. Their results revealed that, when normalized to surface area, even though the capacities of the TiO_2 particles prepared in this study for arsenic sorption were almost comparable to one another, they were significantly lower than the commercially available H-TiO_2, which may be attributed to the particle characteristics and preparation procedures. However, on unit mass basis, amorphous TiO_2 had much larger capacity for As(V) sorption compared to H-TiO_2 while they had similar adsorption capacities for As(III). The adsorption capacities of different TiO_2 polymorphs were dependent on the sorption site density, surface area (particle size) and crystalline structure. This study also revealed that the adsorption capacities of S-TiO_2 and H-TiO_2 for As(III) were ~3.5 and ~2.0 times of those for As(V) under neutral conditions, respectively.

2.2.2. Titanate nanotubes

Niu et al. [52] synthesized titanate nanotubes (TNs) from nanosized titania particles with different surface areas (197–312 m^2 g^{-1}) and pore size diameters (2–6 nm) by alkaline hydrothermal method and investigated their adsorption abilities for arsenic. The TNs with high surface area, open tube end and uniform tubular size exhibited fast uptake rate and high adsorption capacity to inorganic arsenic. Batch experiments showed that the adsorption of As(V) was more favored in acid solution, while the uptake of As(III) was preferred in alkaline solution. The maximum adsorption capacities of TN for As(V) and As(III) were 204.1 mg g^{-1} (pH 3.0) and 59.5 mg g^{-1} (pH 7.0), respectively. However, the adsorption capacities of nanosized titania particles (30–50 nm), from which TNs were prepared, for As(V) and As(III) were only 6.15 mg g^{-1} (pH 3.0) and 6.32 mg g^{-1} (pH 7.0), respectively. The significant increase in arsenic adsorption capacity by converting titania particles to TNs should be associated with the great enhancement in the adsorbents' specific surface area. The results presented in this study [52] suggested the potential of TNs as an efficient material for the treatment of arsenic. However, more experimental work is required to evaluate the possible use of TNs under continuous flow conditions.

2.2.3. Hydrous TiO_2

As(III) is generally reported to have low affinity to the surface of various adsorbents compared with As(V) [53]. Thus, a pretreatment of As(III) by oxidizing it to As(V) and/or adjusting the pH value of water before the adsorption process is necessary and recommended for its effective removal from water [10,54,55]. After the adsorption process, the pH value of treated water body needs to be readjusted back to the neutral state. Thus, it is desirable to develop an effective adsorbent for As(III) without the oxidation/pH adjustment, which can largely simplify the treatment process and lower the treatment cost. Xu et al. [56] synthesized hydrous titanium dioxide ($TiO_2 \cdot xH_2O$) nanoparticles by a low-cost one-step hydrolysis process with aqueous $TiCl_4$ solution. These $TiO_2 \cdot xH_2O$ nanoparticles ranged from 3 to 8 nm and formed aggregates with a highly porous structure, resulting in a large surface area and easy removal capability from aqueous environment after the treatment. The adsorption capacity of As(III) on these $TiO_2 \cdot xH_2O$ nanoparticles reached over 83 mg g^{-1} at near neutral pH environment, and over 96 mg g^{-1} at pH 9.0. The high adsorption capacity of the $TiO_2 \cdot xH_2O$ nanoparticles was related to the high surface area, large pore volume, and the presence of high affinity surface hydroxyl groups. The $TiO_2 \cdot xH_2O$ could successfully remove most of the As(III) contamination from natural water samples of Lake Yangzonghai to meet the USEPA standard for arsenic in drinking water with only a relatively low material loading concentration (0.08 g L^{-1}). However, it is necessary to granulate these $TiO_2 \cdot xH_2O$ nanoparticles into micron-sized particles (hundreds of microns) or load them onto highly porous substrates, which could be used in various flow-through water treatment facilities to avoid the dispersion of these nanoparticles into the environment and its possible subsequences on the environment.

Pirilä et al. [57] examined the suitability and efficiency of an industrial titanium dioxide material, an intermediate from TiO_2 manufacturing process, for water treatment applications as an adsorbent for both As(III) and As(V). The Langmuir adsorption capacities of this TiO_2 were 31.8, 32.1, and 25.8 mg g^{-1} for As(III) while those were 33.4, 22.0 and 26.8 mg g^{-1} for As(V) at pH 4, 5 and 6, respectively, indicating that As(III), typically more challenging, was also removed effectively by TiO_2 under acidic conditions without pre-oxidation. The used TiO_2 was a finely divided high surface area powder containing a mixture of titanium hydroxide and anatase TiO_2, thus it had a great adsorption capacity possibly due to the high surface area and the presence of high affinity surface hydroxyl groups.

2.2.4. Granular TiO_2

Bang et al. [58] prepared granular TiO_2 by agglomerating nanocrystalline anatase and evaluated its performance for arsenic removal from groundwater. Batch experimental results showed that the granular TiO_2 adsorbent had a high adsorption capacity for As(V) and As(III) in a neutral pH range and the As(V) adsorption kinetics was faster than As(III). Groundwater containing an average of 39 μg L^{-1} was continuously passed through a filter containing 3 L of granular TiO_2 and approximately 45,000 bed volumes could be treated by the filter before the effluent arsenic concentration increased to 10 μg L^{-1}. The total treated water volumes per weight of adsorbent were about 60,000 L every 1 kg of adsorbent. This study demonstrated that the granular TiO_2 adsorbent was very effective for arsenic removal from groundwater.

Jing et al. [50] synthesized granular TiO_2 with particle size of 0.60–0.25 mm by agglomerating nanocrystalline anatase and studied the competitive adsorption behavior of As(V), As(III), MMA, and DMA on granular TiO_2. The results indicated that DMA had a much lower affinity for TiO_2 than other arsenic species and its adsorption was hindered by the co-existing anions. The authors also employed granular TiO_2 in the filtration experiments to treat groundwater containing an average of 329 μg L^{-1} As(III), 246 μg L^{-1} As(V), 151 μg L^{-1} MMA, and 202 μg L^{-1} DMA. About 11,000, 14,000, and 9900 bed volumes of water had been treated before the As(III), As(V), and MMA concentration in the effluent increased to 10 μg L^{-1}. However, very little DMA was removed in the filtration experiments, further confirming the low affinity of DMA for TiO_2 surface. Thus, DMA should be pre-oxidized to facilitate its removal.

2.2.5. TiO_2-impregnated chitosan beads (TICB)

Though the granulated TiO_2 adsorbent had been used for water treatment application, the adsorption capacity of the nano particles was reduced by the graduation process. Chitosan is a biopolymer that can be formulated into beads and films [59] and behaves as a hydrogel in non-acidic aqueous solutions. Miller and Zimmerman [60] synthesized a TiO_2-impregnated chitosan beads (TICB) which was efficient for total arsenic removal as well as simplified post-treatment. TICB could remove 2198 μg As(III)/g TICB and 2050 μg As(V)/g TICB in standard batch experiments and 6400 μg As(III)/g TICB and 4925 μg As(V)/g TICB when the system was exposed to UV light. The increase in arsenic adsorption capacity of TICB under UV irradiation should be associated with both an increase in TICB surface area and changes on the bead surface. Moreover, TICB could induce oxidation of As(III) to As(V) in the presence of UV light. Miller et al. [61] further examined the influence of pH, TiO_2 loadings, bead size, UV light and water matrix on arsenic removal by TICB and developed a model to predict arsenic adsorption on TICB as functions of pH and TiO_2 loading. Across pH 4–11 in the presence of UV light, this model predicted adsorption capacity with R^2 values of 0.87 and 0.94 for 10% TiO_2 beads and 30% TiO_2 beads, respectively.

2.2.6. Comparison of the adsorption capacities of TiO_2-based adsorbents

The adsorption capacities of TiO_2-based adsorbents tested for inorganic and organic arsenic removal are summarized in Table 2. It is very difficult to directly compare adsorption capacities due to various experimental conditions used in the studies. Adsorption capacities were evaluated at different pHs, temperatures, As concentration ranges, adsorbent doses, and water composition. Some adsorption capacities were computed by the Langmuir isotherm and others were computed from the pseudo-second order kinetics, which made comparisons more complicated to pursue. However, Table 2 reveals that the adsorption of As(V) and As(III) on TiO_2-based adsorbents refutes the conventional wisdom that "As(III) adsorption to oxides is less effective than As(V) adsorption". Many researchers reported that the TiO_2-based adsorbents had similar adsorption capacities for both As(V) and As(III) or even larger adsorption capacity for As(III) than for As(V) under near neutral conditions or acidic conditions [9,51,57]. Table 2 also reveals that the adsorption capacity of TiO_2-based adsorbents generally increases with increasing the specific surface area, decreasing the degree of crystallinity, or incorporating other metals into it.

3. Enhancing arsenic removal by TiO_2

As mentioned above, using TiO_2 photocatalyst, As(III) can be rapidly oxidized to As(V). Moreover, TiO_2 can also be used as a sorbent for arsenic removal. However, the low adsorption capacity and separation problem of TiO_2 powder from aqueous solution usually limited its application in arsenic removal [62]. Therefore, many efforts have been taken to improve the performance of arsenic removal by TiO_2 and to facilitate the application of TiO_2 in real practice.

3.1. Supported-TiO_2 for PCO of As(III)

Direct application of suspended TiO_2 powders in drinking water treatment may be problematic due to the difficulty of separation and recovery of the tiny particles. Supported TiO_2 is one of the choices for field application of the photocatalyst. Many studies have been carried out to immobilize TiO_2 photocatalyst on porous supporting matrices, such as glass, silica gel, metal, ceramics, polymer, thin films, fibres, zeolite, alumina clays, activated carbon, cellulose, reactor walls and others [47]. However, only very few studies have compared the performance of supported TiO_2 and virgin TiO_2 for PCO of As(III). Yao et al. [63] synthesized a composite photocatalyst by loading TiO_2 onto activated carbon fiber (TiO_2/ACF). They determined the effects of calcination temperature, photocatalyst dosage, pH, initial concentration of As(III) and common anions on the oxidation of As(III). Photocatalytic oxidation of As(III) took place in minutes and followed first-order kinetics. 0.80 mg L^{-1} of As(III) could be entirely oxidized to As(V) within 30 min in the presence of 3.0 g L^{-1} photocatalyst and under UV-light irradiation. The oxidation of As(III) occurred in a wide pH range varying from 2 to 10 with the oxidation efficiency increasing markedly with pH. The supported TiO_2 can be used repeatedly and the photocatalytic oxidation property of TiO_2 was only slightly deteriorated by supporting on ACF.

3.2. Combined use of TiO_2-based photooxidation and other adsorbent for As(III) removal

Nguyen et al. [64] investigated the influence of TiO_2 (as photocatalyst) concentration on As(III) oxidation by photooxidation and found that photooxidation of As(III) to As(V) was possible within minutes at high TiO_2 dosage. In the presence of the TiO_2 photocatalyst, even at a low TiO_2 concentration (0.05 g L^{-1}), the oxidation of

Table 2
Arsenic adsorption by TiO_2 or TiO_2-based materials.

TiO_2	Crystal morphology	Properties			Arsenic species	Adsorption capacity		Reference
		Particle size (nm)	Specific surface area ($m^2\ g^{-1}$)	pH_{pzc}		Γ_{max} ($mg\ g^{-1}$)	Reaction conditions	
Hombikat UV100 TiO_2	99% anatase	<10	334	6.2	As(V)	22.5 ± 5.9	pH 4.0, T = 22 ± 3 °C, $[As(V)]_e$ = ~37.5 mg L^{-1}	[34]
					As(III)	43.1 ± 5.2	pH 9.0, T = 22 ± 3 °C, $[As(III)]_e$ = ~31.9 mg L^{-1}	
Degussa P25 TiO_2	~80% anatase, ~20% rutile	~30	~55	6.9	As(V)	4.6 ± 0.7	pH 4.0, T = 22 ± 3 °C, $[As(V)]_e$ = ~37.5 mg L^{-1}	
					As(III)	3.9 ± 2.4	pH 9.0, T = 22 ± 3 °C, $[As(III)]_e$ = ~39.8 mg L^{-1}	
Nanocrystalline TiO_2	NA	6	330	5.8	As(V)	>37.5	pH 7.0 ± 0.1, T = 21–25 °C, $[As(V)]_e$ = 45 mg L^{-1}, adsorbent = 1 g L^{-1}	[9]
					As(III)	>37.5	pH 7.0 ± 0.1, T = 21–25 °C, $[As(III)]_e$ = 45 mg L^{-1}, adsorbent = 1 g L^{-1}	
Degussa P25 TiO_2	~70% anatase, ~30% rutile	30	50	~6.9	As(V)	8.01	pH 3.0, $[As(V)]_0$ = 5.0–30.0 mg L^{-1}, adsorbent = 1 g L^{-1}, T = 25 °C	[35]
						2.65	pH 7.0, $[As(V)]_0$ = 5.0–30.0 mg L^{-1}, adsorbent = 1 g L^{-1}, T = 25 °C	
Degussa P25 TiO_2	80% anatase and 20% rutile	NA	50	6.8	As(V)	11.9	pH ~ 6.8, $[As(V)]_0$ = 0.1–2.0 mg L^{-1}, adsorbent = 0.1 g L^{-1}	[96]
					As(III)	12.9	pH ~ 6.8, $[As(V)]_0$ = 0.1–2.0 mg L^{-1}, adsorbent = 0.1 g L^{-1}	
					MMA	6.5	pH ~ 6.8, $[MMA]_0$ = 0.1–2.0 mg L^{-1}, adsorbent = 0.1 g L^{-1}	
					DMA	2.8	pH ~ 6.8, $[DMA]_0$ = 0.1–2.0 mg L^{-1}, adsorbent = 0.1 g L^{-1}	
Nanocrystalline TiO_2		6	329	5.8	MMA	4.61	pH 6.0, $[MMA]_0$ = 100 μg As L^{-1}, adsorbent = 0.02 g L^{-1}	[50]
					DMA	2.36	pH 6.0, $[DMA]_0$ = 100 μg As L^{-1}, adsorbent = 0.02 g L^{-1}	
TiO_2	Anatase	6.6	287.8	NA	As(V)	30.5	pH 7.0 ± 0.1, $[As(V)]_0$ = 0–80 mg L^{-1}, adsorbent = 1 g L^{-1}	[44]
		7.0	255.9		As(V)	28.0	pH 7.0 ± 0.1, $[As(V)]_0$ = 0–80 mg L^{-1}, adsorbent = 1 g L^{-1}	
		10.5	141.3		As(V)	18.0	pH 7.0 ± 0.1, $[As(V)]_0$ = 0–80 mg L^{-1}, adsorbent = 1 g L^{-1}	
		14.8	96.0		As(V)	9.86	pH 7.0 ± 0.1, $[As(V)]_0$ = 0–80 mg L^{-1}, adsorbent = 1 g L^{-1}	
		30.1	25.7		As(V)	3.62	pH 7.0 ± 0.1, $[As(V)]_0$ = 0–80 mg L^{-1}, adsorbent = 1 g L^{-1}	
TiO_2	Anatase	6.6	287.8	NA	As(III)	30.0	pH 7.0 ± 0.1, $[As(III)]_0$ = 0–80 mg L^{-1}, adsorbent = 1 g L^{-1}	
		7.0	255.9		As(III)	25.4	pH 7.0 ± 0.1, $[As(III)]_0$ = 0–80 mg L^{-1}, adsorbent = 1 g L^{-1}	
		10.5	141.3		As(III)	15.1	pH 7.0 ± 0.1, $[As(III)]_0$ = 0–80 mg L^{-1}, adsorbent = 1 g L^{-1}	
		14.8	96.0		As(III)	8.52	pH 7.0 ± 0.1, $[As(III)]_0$ = 0–80 mg L^{-1}, adsorbent = 1 g L^{-1}	
		30.1	25.7		As(III)	2.16	pH 7.0 ± 0.1, $[As(III)]_0$ = 0–80 mg L^{-1}, adsorbent = 1 g L^{-1}	
Amorphous TiO_2	Amorphous		409	4.5	As(III)	66.8	pH 7.0, $[As(V)]_0$ = 0.2–50.0 mg L^{-1}, adsorbent = 0.2 g L^{-1}	[51]
					As(V)	19.0	pH 7.0, $[As(III)]_0$ = 0.2–50.0 mg L^{-1}, adsorbent = 0.2 g L^{-1}	
Crystalline TiO_2 from Hydroglobe Inc., NJ	Anatase		98	4.8	As(III)	38.4	pH 7.0, $[As(V)]_0$ = 0.2–50.0 mg L^{-1}, adsorbent = 0.2 g L^{-1}	
					As(V)	19.7	pH 7.0, $[As(III)]_0$ = 0.2–50.0 mg L^{-1}, adsorbent = 0.2 g L^{-1}	
Titanate nanotubes (TN-1)		13	312.59	4.8	As(V)	204.1	pH 3.0, T = 25 °C, $[As(V)]_0$ = 1–500 mg L^{-1}, adsorbent = 1 g L^{-1}	[52]
					As(III)	59.5	pH 7.0, T = 25 °C, $[As(III)]_0$ = 0.1–200 mg L^{-1}, adsorbent = 1 g L^{-1}	
Titania particle	Rutile and anatase	40–50	15.63	6.3	As(V)	6.15	pH 3.0, T = 25 °C, $[As(V)]_0$ = 1–500 mg L^{-1}, adsorbent = 1 g L^{-1}	[52]
					As(III)	6.32	pH 7.0, T = 25 °C, $[As(III)]_0$ = 0.1–200 mg L^{-1}, adsorbent = 1 g L^{-1}	
Hydrous titanium dioxide	Anatase	3–8	312	3.8	As(III)	83	pH 7.0, $[As(III)]_0$ = 0–170.0 mg L^{-1}, adsorbent = 0.5 g L^{-1}	[56]
						96	pH 9.0, $[As(III)]_0$ = 0–190.0 mg L^{-1}, adsorbent = 0.5 g L^{-1}	
Hydrous titanium dioxide		10.8	280	4.8	As(V)	33.4	pH 4.0, $[As(V)]_0$ = 0.2–8.5 mg L^{-1}, T = 20–23 °C	[57]
					As(III)	31.8	pH 4.0, $[As(III)]_0$ = 0.2–8.5 mg L^{-1}, T = 20–23 °C	

Table 2 (*Continued*)

TiO_2	Crystal morphology	Properties			Arsenic species	Adsorption capacity		Reference
		Particle size (nm)	Specific surface area ($m^2\,g^{-1}$)	pH_{pzc}		Γ_{max} ($mg\,g^{-1}$)	Reaction conditions	
Granular TiO_2		0.15–0.6 mm	250.7	5.8	As(V)[a]	41.4	pH 7.0, $[As(V)]_0$ = 0.4–80.0 $mg\,L^{-1}$, adsorbent = 1.0 $g\,L^{-1}$	[58]
					As(III)[a]	32.4	pH 7.0, $[As(III)]_0$ = 0.4–80.0 $mg\,L^{-1}$, adsorbent = 1.0 $g\,L^{-1}$	
					As(V)[b]	40.0	pH 7.0, $[As(V)]_0$ = 0.4–80.0 $mg\,L^{-1}$, adsorbent = 1.0 $g\,L^{-1}$	
					As(III)[b]	39.2	pH 7.0, $[As(III)]_0$ = 0.4–80.0 $mg\,L^{-1}$, adsorbent = 1.0 $g\,L^{-1}$	
TiO_2-impregnated chitosan beads	Anatase	<25 nm	0.56 (without UV irradiation)	7.25	As(V)	2.05	pH 7.7, $[As(V)]_0$ = 0.01–10.0 $mg\,L^{-1}$, adsorbent = 0.625 $g\,L^{-1}$, T = 25 °C	[60]
					As(III)	2.10	pH 9.2, $[As(III)]_0$ = 0.01–10.0 $mg\,L^{-1}$, adsorbent = 0.625 $g\,L^{-1}$, T = 25 °C	
		<25 nm	3.06 (with UV irradiation)	7.25	As(V)	2.99	pH 7.0, $[As(V)]_0$ = 0.01–10.0 $mg\,L^{-1}$, adsorbent = 0.625 $g\,L^{-1}$, T = 25 °C	
					As(III)	3.54	pH 6.6, $[As(III)]_0$ = 0.01–10.0 $mg\,L^{-1}$, adsorbent = 0.625 $g\,L^{-1}$, T = 25 °C	
Ce—Ti oxide	Crystalline CeO_2 amorphous TiO_2	100–200	137	6.2	As(V)	45.0	pH 6.0, $[As(V)]_0$ = 0.1–200 $mg\,L^{-1}$, adsorbent = 0.1 $g\,L^{-1}$, T = 25 °C	[74]
					As(V)	40.2	pH 6.0, $[As(V)]_0$ = 0.1–200 $mg\,L^{-1}$, adsorbent = 0.1 $g\,L^{-1}$, T = 15 °C	
Ce—Ti oxide	Crystalline CeO_2 amorphous TiO_2	100–200	137	6.2	As(V)	44.9	pH 6.5, $[As(V)]_0$ = 0.02–20 $mg\,L^{-1}$, adsorbent = 0.1 $g\,L^{-1}$, T = 25 °C	[75]
					As(III)	55.3	pH 6.5, $[As(III)]_0$ = 0.02–20 $mg\,L^{-1}$, adsorbent = 0.1 $g\,L^{-1}$, T = 25 °C	
Fe—Ti oxide	Fe_3O_4 γ-FeOOH anatase	11.0	77.8	6.0	As(V)	14.0	pH 7.0 ± 0.1, $[As(V)]_0$ = 5.0–250 $mg\,L^{-1}$, adsorbent = 2.0 $g\,L^{-1}$, T = 30 °C	[76]
					As(III)	85.0	pH 7.0 ± 0.1, $[As(III)]_0$ = 5.0–250 $mg\,L^{-1}$, adsorbent = 2.0 $g\,L^{-1}$, T = 30 °C	

[a] In new Jersey groundwater.
[b] In simulated Bangladesh.

As(III) to As(V) was very fast with more than 95% of As(III) getting oxidized to As(V) within 10 min. Although As(III) was assumed to be oxidized to As(V) and then adsorbed on the photocatalyst, some of As(III) might also been adsorbed directly onto the photocatalyst. Therefore, to improve the efficiency of this process, nano-scale zero valent iron (nZVI) was dosed into the photo-reactor. The application of 0.05 $g\,L^{-1}$ nZVI could reduce the TiO_2 requirement by 80% to achieve similar As(III) removal efficiency. However, the authors did not examine the mechanisms of As(III) removal in photocatalysis-nZVI hybrid system extensively.

Taking advantage of the photocatalytic ability of TiO_2 and adsorption capacity of activated alumina (AA), Nakajima et al. [65] proposed to remove As(III), MMA, and DMA from water by the combined use of TiO_2-photocatalyst and AA under photo-irradiation. When an aqueous solution of As(III) (10 mg As L^{-1}) was stirred in the presence of both 1.0 TiO_2 and 1.0 $g\,L^{-1}$ AA under sunlight irradiation, the arsenic removal increased with time and reached 89% after 24 h. By use of the same photocatalyst-adsorbent system, 98% of MMA and 97% of DMA were removed. Yoon and Lee [66] also proposed combining photochemical oxidation and AA for removal of dissolved As(III). The application of UV/TiO_2 process could significantly enhanced arsenic removal by AA from As(III)-contaminated groundwater.

Fostier et al. [67] proposed to remove arsenic from water by immobilizing TiO_2 in PET (polyethylene terephthalate) bottles in the presence of natural sunlight and iron salts. The final conditions (TiO_2 concentration of the coating solution: 10%; Fe(II): 7.0 $mg\,L^{-1}$; solar exposure time: 120 min) were applied to natural water samples spiked with 500 $\mu g\,L^{-1}$ As(III) in order to verify the influence of natural water matrix. After treatment, total As concentration was reduced to lower than 2 $\mu g\,L^{-1}$, showing a removal over 99%, and giving evidence that As(III) was effectively oxidized to As(V). The results obtained demonstrated that TiO_2 could be easily immobilized on a PET surface in order to perform As(III) oxidation in water and that this TiO_2 immobilization, combined with coprecipitation of arsenic on Fe(III) hydroxides(oxides) could be an efficient way for inorganic arsenic removal from groundwater.

3.3. TiO_2-based bimetal adsorbents

To increase the sorption capacity of arsenic, some bimetal oxide adsorbents were prepared [68–72]. It has been reported that the incorporation of La(III), Ce(IV), and Zr(IV) oxides as well as MnO_2 into the adsorbents can significantly increase the sorption capacity of arsenic on the hybrid adsorbents [71,73]. Rare earth oxides were found to effectively remove arsenic due to their relatively small ionic potential and strong basicity [71]. Different metals may also be incorporated into TiO_2 to formulate good adsorbent for arsenic removal. Deng et al. [74] synthesized metal (Al-, Fe-, Ce-, Zr-, La-) doped TiO_2 adsorbents through either precipitation or hydrolysis-precipitation method. The Ce—Ti oxide adsorbent prepared by the hydrolysis-precipitation had the highest adsorption capacity for As(V) than other adsorbents synthesized in their study. The authors also optimized the preparation conditions including the Ti/Ce molar ratio and polyvinyl alcohol (PVA) content. The highest sorption capacity of 45.5 $mg\,g^{-1}$ was achieved at the Ti/Ce molar ratio of 1/1 and PVA content of 0.16%, which was much higher than that of the pure CeO_2 and TiO_2 adsorbents. The Ce—Ti adsorbent exhibited high sorption capacity for As(V) at pH below 7. Column studies showed that about 72,085 bed volumes of As(V) solution at the concentration of 50 $\mu g\,L^{-1}$ and pH 6.5 were filtered when As(V) concentration in the effluent increased to 10 $\mu g\,L^{-1}$, and the average sorption capacity of As(V) on the Ce—Ti adsorbent was about 9.4 $mg\,g^{-1}$. The authors noted that the Ce—Ti oxide adsorbent had the highest sorption capacity at As(V) concentration of 10 $\mu g\,L^{-1}$ among the comparable adsorbents, which was beneficial to the application of Ce—Ti oxide at low As(V) concentration. Deng and co-workers [75] also

compared As(V) and As(III) adsorption on Ce—Ti hybrid oxide adsorbent and reported that the powdered adsorbent had high sorption capacity up to 7.5 mg g^{-1} for As(V) and 6.8 mg g^{-1} for As(III) at the equilibrium arsenic concentration of 10 μg L^{-1}, higher than most reported adsorbents. The optimum adsorption capacity on the adsorbent was achieved at pH below 7 for As(V) and at neutral pH for As(III).

Gupta and Ghosh [76] synthesized hydrous and nanostructured iron(III)—titanium(IV) bimetal oxide (NHITO) and examined As(III) and As(V) adsorption on NHITO at pH 7.0 (±0.1). The kinetic sorption data, in general, for As(III) followed the pseudo-first order while that for As(V) followed the pseudo-second order equation. The adsorption capacities of NHITO for As(III) and As(V) were 85.0 (±4.0) and 14.0 (±0.5) mg g^{-1}, respectively, e.g., the Langmuir sorption capacity of As(III) was nearly six times greater than the As(V). Compared to crystalline hydrous TiO_2 [77] and nano-TiO_2 [9], NHITO had much higher adsorption capacity for As(III) and thus may be applicable in treatment of As(III)-contaminated groundwater. D'Arcy et al. [78] also prepared TiO_2—Fe_2O_3 bi-composite and determined kinetics and isotherms of As(V) adsorption on this bi-composite. Their results revealed that the adsorption capacity of TiO_2—Fe_2O_3 for As(V) at pH 5.0 or 7.0 was about two times of that of pure TiO_2 for As(V) under same conditions. However, the incorporation of Fe_2O_3 into TiO_2 had little enhancement on its adsorption capacity for As(V) at pH 9.0.

3.4. TiO_2-based bifunctional materials

Zhang and Itoh [79] synthesized slag-iron oxide-TiO_2 adsorbent, which could rapidly oxidize As(III) to As(V) and simultaneously remove the As(V) from aqueous solution. The adsorbent was of big size with TiO_2 doped on the surface, which was easy to operate and separate in contaminated water treatment. Loading 10% TiO_2 on the adsorbent was sufficient for the photocatalysis, but the surface area and the adsorption capacity of the adsorbent reduced compared to the adsorbent without TiO_2. A concentration of 100 mg L^{-1} As(III) could be entirely oxidized to As(V) within 3 h in the presence of the adsorbent and under UV-light irradiation, but the equilibrium adsorption of the generated As(V) needed 10 h. The optimum pH value for the oxidation and adsorption was proposed to be around 3. To oxidize and remove original 20 mg L^{-1} or 50 mg L^{-1} As(III) from aqueous solution, the necessary adsorbent amount was 2 g L^{-1} or 5 g L^{-1}, respectively.

Bifunctional mesoporous TiO_2 (*meso*-TiO_2)/α-Fe_2O_3 composites were successfully synthesized by impregnation of Fe^{3+} into *meso*-TiO_2 followed by calcination at 300 °C [80]. The "bifunctional" meant that the composites possessed synergy of the photocatalytic ability of *meso*-TiO_2 for oxidation of As(III) to As(V) and the adsorption performance of α-Fe_2O_3 for As(V). Experimental results showed that the *meso*-TiO_2/α-Fe_2O_3 composites could oxidize As(III) to As(V) with high efficiency at various pH values in the photocatalysis reaction. The highest efficiency of PCO of As(III) was reached when the loading amount of α-Fe_2O_3 was about 50 wt.%. Meanwhile, As(V) could be effectively removed by adsorption onto the surface of composites. Therefore, As(III) could be removed efficiently at various pH values. The excellent adsorption property of α-Fe_2O_3 combining with good photocatalytic ability of *meso*-TiO_2 was very important for the PCO of As(III) and the complete removal of As(V). Moreover, As(V) could be easily desorbed from the composites by heat treatment in alkali solution and the structure of the composites was not destroyed. The resultant composites that possessed the excellent adsorption and desorption performance were very stable even after 8 times recycle.

3.5. Enhancing arsenic removal by TiO_2 with divalent metal ions

Jezequel and Chu [81] carried out a preliminary study to examine the effects of divalent cations on the adsorption of As(V) by TiO_2 nanoparticles. The authors showed that the relatively low As(V) uptake at neutral pH could be substantially enhanced by the addition of common divalent cations such as magnesium and calcium. At equimolar concentrations of cation and As(V) (0.267 mmol L^{-1} each), As(V) adsorption was increased by 83% and 109% in the presence of magnesium and calcium, respectively. At the 1:10 As(V) to cation ratio, the adsorption of As(V) was increased by approximately 200%. This cooperative effect suggested that the uptake capacity of TiO_2 could be effectively utilized in remediating natural waters contaminated with As(V) without the need for pH adjustments.

4. Influence of co-existing solutes on arsenic removal by TiO_2

Competition for sorption sites by silicate, phosphate, carbonate oxyanions and humic acid (HA) appear to sustain elevated aqueous As levels in groundwater [83]. These solutes are often present in arsenic contaminated groundwater, which may affect arsenic removal by TiO_2 either through interfering the photocatalytic oxidation process or compete with arsenic for adsorption process.

4.1. Influence of co-existing solutes on TiO_2 photocatalyzed oxidation of As(III) or organic arsenic

Only very few studies examined the influence of co-existing solutes on TiO_2 photocatalyzed oxidation of As(III) or organic arsenic. Arsenic-contaminated groundwater often contains high levels of iron and dissolved organic carbons. Therefore, Lee and Choi [37] determined the influence of HA and Fe^{3+} on As(III) oxidation in UV-illuminated TiO_2 suspension. Their results revealed that the addition of HA significantly increased the As(III) oxidation rate at pH 3 but had negligible influence at pH 9. The addition of ferric ions to TiO_2 suspension dramatically enhanced the initial As(III) oxidation rate at initial pH 3. Tsimas et al. [43] also investigated the influence of HA on As(III) photooxidation with TiO_2 as catalyst under O_2-saturated conditions and reported that the presence of HA decreased As(III) oxidation rate, which may be associated with the competition between As(III) and HA for the available photogenerated oxidizing species (i.e. valence band holes, hydroxyl radicals and other reactive oxygen species). The different effects of HA on PCO of As(III) reported by different researchers may be ascribed to the different structures of reactors and different operation conditions employed in their studies.

Ferguson et al. [33] reported that addition of phosphate at 0.5–10 μM had little effect on either As(III) sorption or its photooxidation rate but did inhibit adsorption of As(V). Bicarbonate is a well-known $HO^{\bullet}$ scavenger and is present in surface and ground waters at concentrations typically in a range of 50–200 mg L^{-1} [84]. The presence of bicarbonate significantly decreased the rate of MMA degradation [15]. When bicarbonate was 100 and 200 mg L^{-1} and after 72 h of reaction, the MMA concentration was decreased from 10 to 6.1 and 7.1 mg L^{-1}, respectively. The first order rate constant was decreased from 3.3×10^{-2} h^{-1} for the control system to 7.1×10^{-3} and 5.1×10^{-3} h^{-1} for the 100 and 200 mg L^{-1} of bicarbonate systems, respectively. Higher concentrations of bicarbonate caused greater reductions in the rate of MMA degradation.

4.2. Influence of competing ions on arsenic adsorption on TiO_2 based adsorbents

Bang et al. [58] revealed that silica (20 mg L^{-1}) and phosphate (5.8 mg L^{-1}) had no obvious effect on the adsorption capacities of TiO_2 for As(V) and As(III) at neutral pH. Pena et al. [9] compared As(V) and As(III) removal with TiO_2 suspensions prepared in a 0.04 M NaCl solution and in a challenge water containing the competing anions phosphate, silicate, and carbonate. The presence of competing anions considerably reduced As(V) removal and As(III) removal in air-sunlight system at pH > 8.5. The maximum removal of As(III) in N_2 – dark and air – dark systems was reduced from about 95% in the NaCl solution to about 65% in the challenge water. The maximum adsorption pH shifted from about 9 in the NaCl solution to 7.5 in the challenge water, indicating that the adverse effect of the competing anions on As(III) adsorption was more dramatic in a high pH range.

Jézéquel and Chu [35] reported that addition of phosphate resulted in a significant reduction in As(V) adsorption, indicating that phosphate competed with As(V) for the same surface binding sites. By contrast, bicarbonate had little effect on As(V) adsorption, whereas sulfate exhibited a moderate suppression effect. A considerable reduction in As(V) adsorption was also observed in the presence of relatively high concentrations of background electrolytes (>50 mmol L^{-1}).

Liu et al. [85] systematically examined the influence of natural organic matter (NOM) on arsenic adsorption by a commercial available TiO_2 (Degussa P25) in various simulated As(III)-contaminated raw waters. The batch adsorption experiments were conducted under anaerobic conditions and in the absence of light. The presence of 8 mg C L^{-1} NOM in the simulated raw water significantly reduced the amount of arsenic adsorbed at the steady-state. Without NOM, arsenic adsorption increased with increasing solution pH within the pH range of 4.0–9.4. With four of the NOMs tested, arsenic adsorption firstly increased with increasing pH and then decreased after the adsorption reached the maximum at pH 7.4–8.7. An appreciable amount of As(V) was detected in the filtrate after the TiO_2 adsorption in the simulated raw waters that contained NOM, especially at pH > 7. This study suggested that in an As(III)-contaminated raw water, NOM could hinder the uptake of arsenic by TiO_2 by competing with arsenic for the adsorption sites, but could facilitate the As(III) oxidation to As(V) at TiO_2 surface under alkaline conditions and in the absence of O_2 and light.

The influence of ionic strength, electrolyte type (NaCl or $NaClO_4$), and NOM on As(V) adsorption by a commercially available TiO_2 (Degussa P25) was investigated by Liu et al. [86]. As(V) adsorption onto TiO_2 increased with the increase of ionic strength under alkaline conditions (pH 7.0–11.0). Under acidic conditions (pH 4.0–6.0), the adsorption of As(V) onto TiO_2 was insensitive to ionic strength in $NaClO_4$ electrolyte but decreased with increasing ionic strength in NaCl electrolyte. The presence of 2–15 mg L^{-1} NOM as C significantly decreased the fraction of As(V) adsorbed onto TiO_2 at pH 6.0 regardless of the initial As(V) concentration (1–15 μM).

Niu et al. [52] reported that the adsorption capacity of As(V) on TN (180-1) was decreased by 12.5%, 11% and 9% in the presence of phosphate (5 mg L^{-1}), silicate anions (20 mg L^{-1}) and sulfate (50 mg L^{-1}) separately; while no evidently competitive effects on the adsorption of As(III) onto TN (180-1) were observed with these coexisting anions. But for TN (180-2) and titania particle, the adsorption capacity of arsenic was affected clearly in the presence of anions. With the spiked phosphate, silicate anions, the adsorption capacities of As(III) on nanofiber and titania particle were dropped to 60–70% or 65–85% respectively; and for As(V), a decrease of 35–40% or 50–60% of adsorption capacity were observed on the two adsorbents separately.

Jegadeesan et al. [51] reported that the presence of 7 mg L^{-1} phosphate or 20 mg L^{-1} silicate decreased As(III) removal on amorphous TiO_2 by ~43.0% while their presence reduced As(III) removal on commercial crystalline TiO_2 by 60.7% and 42.3%, respectively. Interestingly, the As(V) adsorption capacity of amorphous TiO_2 was not affected by the presence of 7 mg L^{-1} phosphate but was declined by 29.1% in the presence of 20 mg L^{-1} silicate. On the other hand, the presence of 7 mg L^{-1} phosphate or 20 mg L^{-1} silicate decreased As(V) adsorption capacity on commercial crystalline TiO_2 by 17.5–20.7%.

The effect of phosphate and sulfate ions on arsenic sorption (amount loaded = 5.0 mg g^{-1} sorbent) at pH 7.0 (±0.1) showed no significant effect on As(III) removal by NHITO while those ions have reduced the As(V) removal percentage from 83.0 (±1.5) to 23.4 (±1.1) and 35.0 (±1.0) with increasing mole ratio of (i) PO_4^{3-}:As from 0 to 1.6 and (ii) SO_4^{2-}:As from 0 to 27.3, respectively [76]. The significant interference on As(V) sorption by phosphate and sulfate was due to the similar chemistry of As(V) with phosphate and sulfate in aqueous solution at pH 7.0 (±0.1).

Deng et al. [74] determined the influence of anions such as sulfate, silicate, carbonate, chloride, and phosphate commonly exist in groundwater on the sorption of As(V) on the Ce—Ti oxide adsorbent. These anions at different concentrations (0.1 and 1 mM) had different effects on the sorption. HPO_4^{2-} even at low concentration of 0.1 mM caused the greatest decrease in As(V) sorption among seven anions, which may be attributed to their similar ionization constants and ionic structure. The effect of seven anions on As(V) sorption on the Ce—Ti oxide adsorbent followed the decreasing order of $HPO_4^{2-} > F^- > HCO_3^- > SiO_3^{2-} > SO_4^{2-} \approx NO_3^- > Cl^-$. Fluoride had moderate effect on the adsorption, while sulfate, nitrate, and chloride had little effect even at high concentration of 1 mM. Since fluoride and As(V) are present in some groundwater simultaneously and fluoride concentration is in the range of 1–10 mg L^{-1}, its effect on As(V) sorption is not ignorable.

To sum up, the TiO_2-catalyzed photooxidation of arsenic was strongly influenced by humic acid and bicarbonate generally existing in groundwater. On the other hand, the effect of phosphate, silicate, fluoride, and humic acid on arsenic adsorption by TiO_2-based materials should not be neglected.

5. Mechanisms of arsenic removal by TiO_2

5.1. TiO_2 assisted PCO of As(III) and organic arsenic

Under UV illumination, the TiO_2 photocatalyst absorbs photons with energy equal or higher than its band gap energy (<385 nm, usually UVA is applied), which leads to the formation of electron (conduction band) and hole (valence band) pair (reaction (1) in Table 3) [33,40]. In the absence of an electron or hole trap, recombination of the e_{CB}^-/h_{VB}^+ pair occurs via thermal decay (reaction (2) in Table 3) [33,40]. In aerated aqueous suspensions, oxygen acts as an electron trap leading to superoxide anion radical ($O_2^{\bullet -}$, reaction (3) in Table 3), prolonging the lifetime of hole, which subsequently leads to the formation of the surface associated hydroxyl radicals ($^\bullet$OH, reaction (4) in Table 3). The generated superoxide and hydroxyl radicals may undergo a series conversion with the e_{CB}^-/h_{VB}^+ pair and H^+ (reactions (5)–(9) in Table 3) [87]. The redox potential of the As(V)/As(III) couple is lower than the valence band potential so the photo-generated holes have enough thermodynamic potential to oxidize As(III) to As(V) [88]. Thus, TiO_2 photocatalysis has been shown to be effective in oxidizing As(III) to As(V) with oxygen in many studies as discussed in Section 2.1. Although the PCO of As(III) has been shown to be robust over a wide pH range, the mechanism of PCO of As(III) remains as a controversial issue. The oxidation of As(III) occurs through a

Table 3
Major reactions involved in TiO_2-photocatalyzed As(III) oxidation.

Reactions		Reference
Generation of charge carriers and photooxidants		
$TiO_2 + h\nu \rightarrow e^-_{CB} + h^+_{VB}$	(1)	[33,36]
$e^-_{CB} + h^+_{VB} \rightarrow$ heat	(2)	
$O_2 + e^-_{CB} \rightarrow O_2^{\bullet -}$	(3)	
$OH_{ads} + h^+_{VB} \rightarrow {}^\bullet OH$	(4)	
$O_2^{\bullet -} + H^+ \rightarrow HO_2^\bullet$	(5)	
$O_2^{\bullet -} + 2H^+ + e^-_{CB} \rightarrow H_2O_2$	(6)	
$H_2O_2 + e^-_{CB} \rightarrow {}^\bullet OH + OH^-$	(7)	
$H_2O_2 + h^+_{VB} \rightarrow HO_2^\bullet + H^+$	(8)	
$2O_2^{\bullet -} + 2H^+ \rightarrow H_2O_2 + O_2$	(9)	
As(III) as a charge recombinant		
$As(III) + {}^\bullet OH/h^+_{VB} \rightarrow As(IV)$	(10)	[29,82]
$As(IV) + e^-_{CB} \rightarrow As(III)$	(11)	
As(III) oxidation		
Superoxide as the oxidant		
$As(III) + O_2^{\bullet -}/HO_2^\bullet \rightarrow As(IV) \xrightarrow{O_2} As(V)$	(12)	[29,37,39]
$As(III) + 2HO_2^\bullet \rightarrow As(V) + 2OH^- + O_2$	(13)	
Positive hole as the oxidant		
$As(III) + h^+_{VB} \rightarrow As(IV) \xrightarrow{VB\ holes} As(V)$	(14)	[38,87]
Hydroxyl radicals as the oxidant		
$As(III) + {}^\bullet OH \rightarrow As(IV) + OH^- \xrightarrow{O_2} As(V)$	(15)	[40,91]

transient species (i.e., As(IV)). Because the As(IV) is readily oxidized to As(V) even by oxygen ($k(As(IV)+O_2) = 1.1 \times 10^9\ M^{-1}\ s^{-1}$) [89], it is important to know which species (h_{vb}^+, $^\bullet OH$, or $HO_2^\bullet/O_2^{\bullet -}$) is mainly responsible for the rate-determining step (As(III) → As(IV)). So far, different opinions have been proposed on this issue. Valence band (VB) hole, $^\bullet OH$ radical, or superoxide may initiate the oxidation of As(III) following one of the reactions (12)–(15) presented in Table 3. The various TiO_2-catalyzed As(III)/organic arsenic photooxidation pathways are illustrated in Fig. 3.

5.1.1. Superoxide as the main oxidant of As(III)

Choi and his colleagues have carried out a series of studies to confirm the superoxide mediated As(III) oxidation mechanism in the UV/TiO_2 process [29,37,39,90]. Lee and Choi [37] performed the PCO of As(III) in aqueous TiO_2 suspension and reported that As(III) oxidation in UV-illuminated TiO_2 suspension was highly efficient in the presence of dissolved oxygen. Since the addition of excess tert-butyl alcohol ($^\bullet OH$ radical scavenger) did not reduce the rate of As(III) oxidation, the $^\bullet OH$ radicals should not be responsible for As(III) oxidation. The authors proposed that the superoxide was the main oxidant of As(III) in the TiO_2/UV process. Ryu and Choi [39] synthesized TiO_2, Pt-TiO_2, and fluorinated TiO_2 and determined the As(III) oxidation rate in TiO_2 or modified TiO_2 photocatalytic systems to confirm that superoxides were mainly responsible for the As(III) PCO. The rate of As(III) oxidation drastically increased on Pt-TiO_2, which could be ascribed to the enhanced superoxide generation through an efficient interfacial electron transfer from the conduction band (CB) to O_2. Since the addition of tert-butyl alcohol had little effect on the PCO rate in both naked and Pt-TiO_2 suspensions, $^\bullet OH$ radicals did not seem to be involved in As(III) oxidation. Fluorinated TiO_2 that had a markedly reduced adsorptive capacity for As(III) did not show a reduced PCO rate, which indicated that the direct hole transfer path was not important. The As(III) oxidation proceeded under visible light with a similar rate to the case of Pt-TiO_2/UV when dye-sensitized Pt-TiO_2 was used. Since only superoxides could be generated as a photooxidant in this visible light system, their role as a main oxidant of As(III) was confirmed. The significant decrease in PCO rate caused by the presence of superoxide dismutase further confirmed the important role of superoxides in As(III) oxidation.

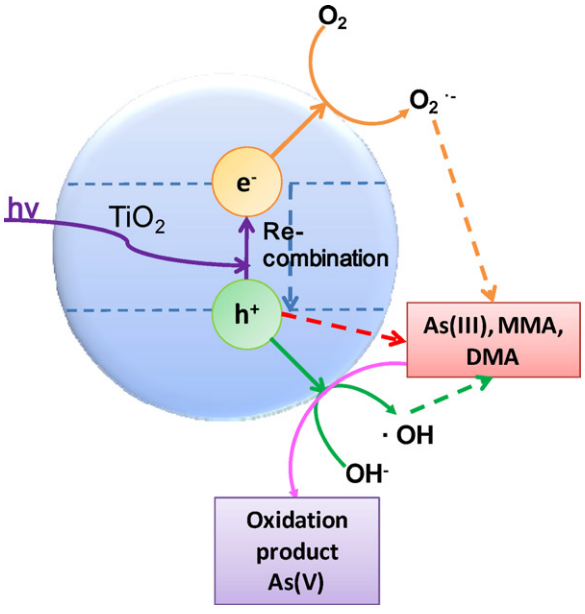

Fig. 3. Schematic illustration of TiO_2-catalyzed As(III)/organic arsenic photooxidation pathways.

Ferguson et al. [33] observed that compared to air-purged samples, the As(III) PCO was inhibited almost entirely by sparging with N_2 and addition of CCl_4 as an alternate electron acceptor for O_2, indicating that oxidation of As(III) by holes or surface-bound $^\bullet OH$ radicals did not occur to a significant degree in this system. Moreover, As(III) photooxidation in the presence of superoxide dismutase confirmed the observations of Ryu and Choi [39] and supported their hypothesis that $O_2^{\bullet -}$ played a major role in As(III) photooxidation [33].

Ryu and Choi [90] proposed that the adsorbed As(III) on TiO_2 served as an external charge-recombination center where the reaction of As(III) with an $^\bullet OH$ radical (or hole) was immediately followed by an electron transfer to make a null cycle (reactions (10) and (11) in Table 3). Under such conditions, superoxides that are much longer lived and are able to diffuse farther into the bulk solution govern the overall oxidation process. Moreover, the concentration of superoxides generated in the illuminated TiO_2 suspension should be high enough to account for the observed rate of As(V) generation although the intrinsic reactivity of superoxides with As(III) is lower than that of $^\bullet OH$ radicals by 3 orders of magnitude. This was confirmed by the observation that the photoanodic current obtained with a TiO_2 electrode immediately decreased upon spiking with As(III), portraying the superoxide-mediated PCO as the dominant pathway.

Choi et al. [29] further provided direct evidence to support the role of As(III) in the charge recombination dynamics using time-resolved transient absorption spectroscopy. The presence of As(III) indeed mediated the charge recombination in TiO_2 (reactions (10) and (11) in Table 3). Under this condition, the role of the $^\bullet OH$ radical was suppressed because of the null cycle, and the weaker oxidant superoxide, should prevail. The role of the superoxide had been previously doubted on the basis of the observation that the addition of excess formic acid (hole scavenger that should enhance the production of superoxides) inhibited the PCO of As(III). However, Choi et al. [29] proved that this was due to the photogeneration of reducing radicals ($HCO_2^\bullet$) that recycled As(V)/As(IV) back to As(III).

5.1.2. Direct hole oxidation mechanism

Since the rate constant of As(III) oxidation by $^\bullet OH$ is about 3 orders of magnitude higher than that of As(III) oxidation by $O_2^{\bullet -}$ [89], the proposal by Choi and his colleagues that superoxide is the

primary oxidant of As(III) to As(VI) [37,39] is unusual because it is well accepted that •OH radicals are main oxidants in most TiO_2-mediated PCO processes. This claim has been doubted and refuted by other research groups, who hold that TiO_2 PCO reactions are always initiated by VB hole (VB hole, h_{VB}^+) or adsorbed •OH radical.

Jayaweera et al. [38] observed that when N_2 was purged in place of air through the sample during UV irradiation, rate of depletion of As(III) dropped appreciably, suggesting that dissolved oxygen played an important role in the PCO of As(III). Thus they proposed that As(III) was oxidized by the positive holes generated.

Yoon and Lee [87] performed a series of As(III) oxidation experiments by using UV-C/H_2O_2 and UV-A/TiO_2 to investigate the TiO_2-photocatalyzed oxidation mechanism of As(III). The experiment with UV-C/H_2O_2 indicated that HO_2•/O_2•$^-$ was not an effective oxidant of As(III) in the homogeneous phase. The effects of oxalate, formate, and Cu(II) on the PCO of As(III) contradicted the controversial hypothesis that HO_2•/O_2•$^-$ was the main oxidant of As(III) in the UV/TiO_2 system. The effect of As(III) on the TiO_2-photocatalyzed oxidations of benzoate, terephthalate, and formate was also incompatible with the superoxide-based As(III) oxidation mechanism. Instead, the experimental observations implied that •OH and/or the positive hole were largely responsible for the oxidation of As(III) in the UV/TiO_2 system. Since excess methanol (a scavenger of adsorbed •OH) did not retard the oxidation rate of As(III), •OH seemed not to be the main oxidant. Therefore, the best rationale regarding the oxidation mechanism of As(III) in the UV/TiO_2 system seemed to be the direct electron transfer between As(III) and positive holes.

Yoon et al. [91] carried out further study to investigate the correlation between As(III) oxidation and superoxide in the UV/TiO_2 system, where both As(V) and H_2O_2 were measured simultaneously. When excess formic acid was added as a scavenger of VB hole or •OH in UV/TiO_2 or vacuum-UV lamp irradiation ($\lambda = 185 + 254$ nm), As(III) oxidation was greatly inhibited while H_2O_2 generation was promoted. Since H_2O_2 was photochemically produced through the disproportionation of superoxide, this result definitely showed that superoxide played a little role in the oxidation of As(III) not only in UV/TiO_2 but also in other advanced oxidation processes (AOPs). Interestingly, not only formic acid but also methanol showed an inhibitory effect on TiO_2 PCO of As(III). Excess methanol retarded the TiO_2 PCO of As(III) moderately but not completely, which indicated that adsorbed •OH also played a significant role along with VB hole in the TiO_2 PCO of As(III). This study provided convincing evidence to support that adsorbed •OH and VB hole were the main oxidants in the TiO_2 PCO of As(III).

Both photoelectrochemical method and As(III) oxidation kinetic measurements were performed to clarify whether superoxide was the main oxidant in the normal air-saturated TiO_2 PCO of As(III) system [92]. Under a sufficient cathodic bias potential, the dark oxidation of As(III) by superoxide could occur, but both the reaction rate and the columbic efficiency were rather low, suggesting that it was a weak oxidant. However, under UV light, both the reaction rate and the columbic efficiency were greatly enhanced even at potentials negative enough to eliminate photohole participation, indicating that more efficient oxidants than superoxide were produced. Under UV illumination and enough positive potential where superoxide was absent, the As(III) oxidation was the most highly efficient. The columbic efficiency of photoholes was much higher than that of superoxide. In the normal aerated aqueous solutions and at open circuit, although the total contribution of superoxide and its derivates to the PCO of As(III) was considerably high (up to 43%), it was not more than that of photohole (57%). Thus, As(III) could be oxidized almost equally highly efficient via both hole- and electron-initiated mechanisms. However, their study cannot demonstrate whether As(III) was oxidized directly by hole or indirectly by hydroxyl radicals by the employed photoelectrochemical method.

5.1.3. OH as the major oxidant

Some other researchers proposed that •OH radicals were the major oxidant contributing to As(III) oxidation in the UV/TiO_2 process. Dutta et al. [40] investigated the PCO of As(III) to As(V) and employed benzoic acid (BA) as a hydroxyl radical scavenger to provide evidence for the •OH as the main oxidant for oxidation of As(III). Formation of salicylic acid (SA) from the oxidation of BA by •OH demonstrated the involvement of •OH in the mechanism of As(III) oxidation. The effect of Fe(III) on As(III) oxidation at different pH values with and without TiO_2 under UV light also suggested that •OH be the dominant oxidant for As(III) oxidation.

Xu et al. [42] assessed the roles of O_2, H_2O_2, •OH, and O_2•$^-$ in the TiO_2 assisted PCO of As(III). When evaluated the oxidation of As(III) by TiO_2 PCO, the authors considered both the dissolved and the adsorbed arsenic species. They used extraction and analyses of the arsenic species adsorbed onto the surface of the TiO_2 to illustrate that the oxidation of As(III) to As(V) occurred in an adsorbed state during TiO_2 PCO. The TiO_2 PCO of surface adsorbed As(III) in deoxygenated solutions with electron scavengers, Cu^{2+}, and polyoxometalates (POM) yielded oxidation rates that were comparable to those observed under oxygen saturation, implying the primary role of oxygen was as a scavenger of the conduction band electron. Pulse radiolysis and competition kinetics were employed to determine a rate constant of $3.6 \times 10^6\ M^{-1}\ s^{-1}$ for the reaction of As(III) with O_2•$^-$, 3 orders magnitude slower than the reaction rate of As(III) oxidation by •OH. Transient absorption studies of adsorbed hydroxyl radicals, generated by subjecting colloidal TiO_2 to radiolytic conditions, provided convincing evidence that the adsorbed hydroxyl radical (TiO_2 + •OH) played the central role in the oxidation with As(III) during TiO_2 assisted photocatalysis. Their results suggested the reaction of O_2•$^-$ did not contribute in the conversion of As(III) when compared to the reaction of As(III) with •OH radical during TiO_2 PCO.

Xu et al. [11] revealed that addition of tert-butyl alcohol during TiO_2 photocatalysis dramatically reduced the rate of degradation of MMA and DMA, indicating that •OH was the primary oxidant. They concluded that the PCO of MMA and DMA led to cleavage of the arsenic carbon bond, ultimately yielding As(V). Radical scavengers, including superoxide dismutase, sodium bicarbonate, tert-butanol, and sodium azide, were used to study the photodegradation mechanisms of MMA and DMA [15]. The results showed that hydroxyl radicals (•OH) was the primary reactive oxygen species for the photodegradation of MMA and DMA. The methyl groups in MMA and DMA were transformed into organic carbon, including formic acid and possibly methanol, also through photochemical reactions.

Zheng et al. [49] explored the roles of reactive oxygen species, •OH, $^1O_2$, O_2•$^-$ and h_{VB}^+ in TiO_2-catalyzed photooxidation of PA by adding appropriate scavengers to the reaction medium and the results suggested that •OH played a major role in the degradation of PA. By-product studies indicated the surface of the catalyst played a key role in the formation of the primary products and the subsequent oxidation pathways led to the mineralization of PA to inorganic arsenic.

5.2. Mechanisms of arsenic adsorption on TiO_2-based adsorbents

Although there has been a controversy over the TiO_2 PCO mechanism of As(III) for the past 10 years. The researchers had general agreement in the adsorption mechanisms of various arsenic species on TiO_2-based adsorbents. Pena et al. [93] employed electrophoretic mobility (EM) measurements, Fourier transform infrared (FTIR) spectroscopy, extended X-ray absorption fine structure (EXAFS) spectroscopy to investigate the As(V) and As(III)

interactions at the solid-water interface of nanocrystalline TiO_2. The adsorption of As(V) and As(III) decreased the point of zero charge of TiO_2 from 5.8 to 5.2, suggesting the formation of negatively charged inner-sphere surface complexes for both arsenic species. The EXAFS analyses indicated that both As(V) and As(III) form bidentate binuclear surface complexes as evidenced by an average Ti—As(V) bond distance of 3.30 Å and Ti—As(III) bond distance of 3.35 Å. The FTIR bands caused by vibrations of the adsorbed arsenic species remained at the same energy levels at different pH values. Consequently, the surface complexes on TiO_2 maintained the same nonprotonated species at pH values from 5 to 10, and the dominant surface species were $(TiO)_2AsO_2^-$ and $(TiO)_2AsO^-$ for As(V) and As(III), respectively.

Jegadeesan et al. [51,94] employed X-ray absorption near edge structure (XANES) and EXAFS to determine the mechanisms of arsenic adsorption on TiO_2 and reported that partial oxidation of As(III) happened when As(III) was adsorbed onto amorphous TiO_2 but no As(III) oxidation occurred when As(III) was adsorbed onto commercial crystalline TiO_2. Their data also indicated that As(III) and As(V) form binuclear bidentate inner-sphere complexes with amorphous TiO_2 at neutral pH. As(V) adsorption on commercial crystalline TiO_2 was also characteristic of a bidentate binuclear complex.

Niu et al. [52] noticed that the adsorption of As(V) and As(III) decreased the pH_{pzc} of titanate nanotubes to approximately 4.3 and 4.0, respectively, implying that the negatively charged inner-sphere complexes between As(V) or As(III) and TNs were formed upon the adsorption of arsenic. There was no As(III) oxidized into As(V) during the adsorption process in their study.

Li et al. [75] investigated the adsorption mechanisms of As(V) and As(III) on Ce—Ti bimetal oxide. The pH_{pzc} shifted from 6.2 to pH 4.4 and pH 4.6 after As(V) and As(III) sorption, respectively, indicating the formation of inner-sphere complexes on the adsorbent. FTIR analysis indicated that the hydroxyl groups on the adsorbent surface were involved in arsenic adsorption, while X-ray photoelectron spectroscopy (XPS) provided further evidence for the involvement of hydroxyl groups in the sorption and the formation of monodentate and bidentate complexes on the adsorbent surface [75].Jing et al. [95] investigated the adsorption mechanisms of MMA and DMA on nanocrystalline TiO_2 with EXAFS. The EXAFS results show that MMA formed bidentate surface complexes on TiO_2 with an As—Ti distance of 3.32 ± 0.01 Å, while DMA formed monodentate complexes with an As—Ti distance of 3.37 ± 0.04 Å. Adsorption of MMA and DMA on TiO_2 shifted the IEP from pH 5.8 to pH 4.1 and 4.8, respectively, indicating the formation of negatively charged surface complexes.

Jing et al. [50] carried out field filtration experiment with granular TiO_2 as the filtration media for 4 months to treat groundwater containing As(V), As(III), DMA and MMA. EXAFS spectroscopy was employed to determine the arsenic local coordination environment for spent adsorbent at 5 cm depth below the surface and at 5 cm above the bottom in the TiO_2 column. The As—O interatomic distance suggested the adsorbed As was in As(V) form and the AsO_4 tetrahedral geometry remained relatively rigid on the TiO_2 surface. The second shell can be fitted with 2.6 and 2.8 Ti atoms at a distance of 3.30 and 3.31 Å for the top and bottom sample, respectively. The distances and coordination numbers (CN) of As—O and As—Ti indicated the formation of a bidentate binuclear As(V) surface complex on TiO_2 adsorbent. The surface As speciation analysis using EXAFS indicated the oxidation of adsorbed As(III) to As(V) in the TiO_2 column. The unidentifiable MMA species on spent TiO_2 may be ascribed to the ambiguity between oxygen and carbon atoms in the As first shell analysis, and to its low abundance compared to the inorganic As species. The complexation between TiO_2 surface and various arsenic species in the pH range of 6.5–8.5 was illustrated in Fig. 4.

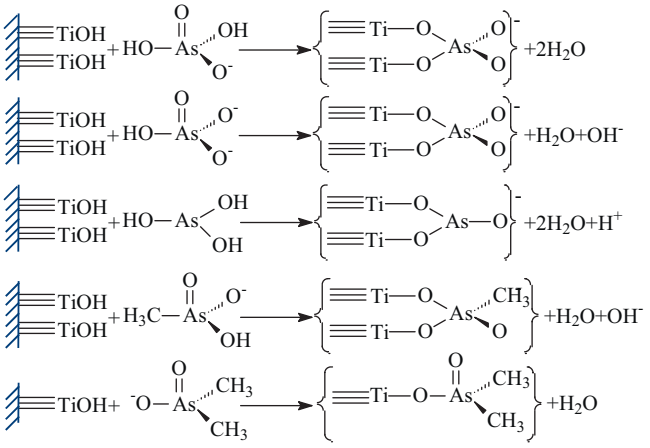

Fig. 4. Schematic illustration of the complexes formed between various arsenic species and TiO_2 surface.

6. Conclusions and future challenges

Extensive arsenic contamination of surface and groundwater has been reported in many parts of the world. The four arsenic species commonly reported are As(III), As(V), MMA and DMA. Despite the fact that inorganic species are predominant in natural waters, the presence of MMA and DMA has also been reported. Elevated levels of arsenic in groundwater not only cause significant problems in the provision of safe drinking water, but lately have also raised concern regarding food safety. This paper reviewed the application of TiO_2 and TiO_2-based materials in removing inorganic and organic arsenic. TiO_2-based arsenic removal methods developed to date have focused on the PCO of As(III)/organic arsenic to As(V) and adsorption of inorganic and organic arsenic. TiO_2 photocatalysis was an effective method for oxidizing As(III)/organic arsenic to As(V) in the presence of oxygen. Although As(III)/organic arsenic can be oxidized to As(V) in the TiO_2/UV system, the adsorption property of TiO_2 is not very good at low absorbent content, resulting in the unefficient removal of As(V). This shortcoming could be overcome by combing TiO_2 with other adsorbents with good adsorption property in one system or developing bifunctional adsorbents with both great photocatalytic ability and high adsorption capacity. The adsorption capacity of TiO_2 can be enhanced by increasing the specific surface area, decreasing the degree of crystallinity, or incorporating other metals into it. Only few studies have been carried out to investigate the influence of co-existing solutes on TiO_2 photocatalyzed oxidation of As(III)/organic arsenic and some results are contradictory. Among the anions which commonly exist in actual groundwater, the effect of phosphate, silicate, fluoride, and humic acid on arsenic adsorption by TiO_2-based materials should not be neglected. There has been a controversy over the TiO_2 PCO mechanisms of As(III) for the past 10 years. The key argument has been whether superoxide ($HO_2^{\bullet}/O_2^{\bullet-}$) or hydroxyl radical or the positive hole is the major oxidant of As(III) in the UV/TiO_2 system. The researchers agreed that inorganic and organic arsenic formed inner sphere complexes with the surface upon their adsorption onto TiO_2-based materials. As(III), As(V), MMA form binuclear bidentate inner-sphere complexes while DMA form mononuclear inner-sphere complexes with TiO_2 at neutral pH.

Future needs in TiO_2-based arsenic removal technology should take into considerations of reducing the treatment cost, decreasing the operational complexity of the technology and disposal of arsenic bearing treatment residual. Specifically, studies should be carried out to:

(1) design new and inexpensive bi-functional materials based on TiO_2, which hold a high photo-efficiency that can utilize wider solar spectra and hold a high arsenic adsorption capacity;
(2) synthesize TiO_2-based adsorbents by incorporating other metals into TiO_2 to achieve high adsorption capacity for both As(V) and As(III);
(3) optimize the structure of the photocatalytic reactors to enhance PCO kinetics and to increase the utilization of solar energy to reduce the electricity costs;
(4) clarify the mechanisms of TiO_2 photocatalyzed oxidation of As(III);
(5) implement TiO_2 immobilization strategy to provide a cost-effective solid-liquid separation and carry out more field experiments to promote the application of TiO_2 in practice;
(6) evaluate the safety of As-loaded sludge and determine the proper disposal methods.

Acknowledgements

This work was supported by the National Natural Science Foundation of China (50908060) and State Key Laboratory of Pollution Control and Resources Reuse (PCRRY11001). The authors would like to acknowledge the three anonymous reviewers and Prof. Wonyong Choi for their efforts in helping us to improve this paper.

References

[1] P.L. Smedley, D.G. Kinniburgh, A review of the source, behaviour and distribution of arsenic in natural waters, Appl. Geochem. 17 (2002) 517–568.
[2] M. Bissen, F.H. Frimmel, Arsenic – a review. Part I: Occurrence, toxicity, speciation, mobility, Acta Hydrochim. Hydrobiol. 31 (2003) 9–18.
[3] M. Bissen, F.H. Frimmel, Arsenic – a review. Part II: Oxidation of arsenic and its removal in water treatment, Acta Hydrochim. Hydrobiol. 31 (2003) 97–107.
[4] A. Heikens, G.M. Panaullah, A.A. Meharg, Arsenic behaviour from groundwater and soil to crops: impacts on agriculture and food safety, in: G.W. Ware (Ed.), Reviews of Environmental Contamination and Toxicology, vol. 189, Springer, 2007, pp. 43–87.
[5] T. Appelo (Ed.), Arsenic in Groundwater – a World Problem, Netherlands National Committee of the IAH, Deltares, 2006.
[6] X.G. Meng, S. Bang, G.P. Korfiatis, Effects of silicate, sulfate, and carbonate on arsenic removal by ferric chloride, Water Res. 34 (2000) 1255–1261.
[7] V.K. Sharma, M. Sohn, Aquatic arsenic: toxicity, speciation, transformations, and remediation, Environ. Int. 35 (2009) 743–759.
[8] T.S.Y. Choong, T.G. Chuah, Y. Robiah, F.L.G. Koay, I. Azni, Arsenic toxicity, health hazards and removal techniques from water: an overview, Desalination 217 (2007) 139–166.
[9] M.E. Pena, G.P. Korfiatis, M. Patel, L. Lippincott, X.G. Meng, Adsorption of As(V) and As(III) by nanocrystalline titanium dioxide, Water Res. 39 (2005) 2327–2337.
[10] X.H. Guan, J. Ma, H.R. Dong, L. Jiang, Removal of arsenic from water: effect of calcium ions on As(III) removal in the $KMnO_4$—Fe(II) process, Water Res. 43 (2009) 5119–5128.
[11] T. Xu, Y. Cai, K.E. O'Shea, Adsorption and photocatalyzed oxidation of methylated arsenic species in TiO_2 suspensions, Environ. Sci. Technol. 41 (2007) 5471–5477.
[12] A.J. Bednar, J.R. Garbarino, J.F. Ranville, T.R. Wildeman, Presence of organoarsenicals used in cotton production in agricultural water and soil of the southern United States, J. Agric. Food. Chem. 50 (2002) 7340–7344.
[13] E.M. Kenyon, M.F. Hughes, A concise review of the toxicity and carcinogenicity of dimethylarsinic acid, Toxicology 160 (2001) 227–236.
[14] L.L. Arnold, M. Eldan, A. Nyska, M. van Gemert, S.M. Cohen, Dimethylarsinic acid: results of chronic toxicity/oncogenicity studies in F344 rats and in B6C3F1 mice, Toxicology 223 (2006) 82–100.
[15] Z. Xu, C. Jing, F. Li, X. Meng, Mechanisms of photocatalytical degradation of monomethylarsonic and dimethylarsinic acids using nanocrystalline titanium dioxide, Environ. Sci. Technol. 42 (2008) 2349–2354.
[16] A. Akter, M.H. Ali, Arsenic contamination in groundwater and its proposed remedial measures, Int. J. Environ. Sci. Technol. 8 (2011) 433–443.
[17] X.H. Guan, H.R. Dong, J. Ma, L. Jiang, Removal of arsenic from water: Effects of competing anions on As(III) removal in $KMnO_4$—Fe(II) process, Water Res. 43 (2009) 3891–3899.
[18] B.B. Han, T. Runnells, J. Zimbron, R. Wickramasinghe, Arsenic removal from drinking water by flocculation and microfiltration, Desalination 145 (2002) 293–298.
[19] S. Wang, X. Zhao, On the potential of biological treatment for arsenic contaminated soils and groundwater, J. Environ. Manage. 90 (2009) 2367–2376.
[20] M.J. Kim, J. Nriagu, Oxidation of arsenite in groundwater using ozone and oxygen, Sci. Total Environ. 247 (2000) 71–79.
[21] D. Mohan, C.U. Pittman Jr., Arsenic removal from water/wastewater using adsorbents – a critical review, J. Hazard. Mater. 142 (2007) 1–53.
[22] X.H. Guan, T.Z. Su, J.M. Wang, Quantifying effects of pH and surface loading on arsenic adsorption on NanoActive alumina using a speciation-based model, J. Hazard. Mater. 166 (2009) 39–45.
[23] Y.H. Kim, C.M. Kim, I.H. Choi, S. Rengaraj, J.H. Yi, Arsenic removal using mesoporous alumina prepared via a templating method, Environ. Sci. Technol. 38 (2004) 924–931.
[24] T.F. Lin, J.K. Wu, Adsorption of arsenite and arsenate within activated alumina grains: equilibrium and kinetics, Water Res. 35 (2001) 2049–2057.
[25] X.H. Guan, J.M. Wang, C.C. Chusuei, Removal of arsenic from water using granular ferric hydroxide: macroscopic and microscopic studies, J. Hazard. Mater. 156 (2008) 178–185.
[26] M. Arienzo, P. Adamo, J. Chiarenzelli, M.R. Bianco, A. De Martino, Retention of arsenic on hydrous ferric oxides generated by electrochemical peroxidation, Chemosphere 48 (2002) 1009–1018.
[27] K. Banerjee, G.L. Amy, M. Prevost, S. Nour, M. Jekel, P.M. Gallagher, C.D. Blumenschein, Kinetic and thermodynamic aspects of adsorption of arsenic onto granular ferric hydroxide (GFH), Water Res. 42 (2008) 3371–3378.
[28] O.S. Thirunavukkarasu, T. Viraraghavan, K.S. Subramanian, S. Tanjore, Organic arsenic removal from drinking water, Urban Water 4 (2002) 415–421.
[29] W. Choi, J. Yeo, J. Ryu, T. Tachikawa, T. Majima, Photocatalytic oxidation mechanism of As(III) on TiO_2: unique role of As(III) as a charge recombinant species, Environ. Sci. Technol. 44 (2010) 9099–9104.
[30] D. Nabi, I. Aslam, I.A. Qazi, Evaluation of the adsorption potential of titanium dioxide nanoparticles for arsenic removal, J. Environ. Sci. China 21 (2009) 402–408.
[31] T. Balaji, H. Matsunaga, Adsorption characteristics of As(III) and As(V) with titanium dioxide loaded amberlite XAD-7 resin, Anal. Sci. 18 (2002) 1345–1349.
[32] M.A. Ferguson, J.G. Hering, TiO_2-photocatalyzed As(III) oxidation in a fixed-bed, flow-through reactor, Environ. Sci. Technol. 40 (2006) 4261–4267.
[33] M.A. Ferguson, M.R. Hoffmann, J.G. Hering, TiO_2-photocatalyzed As(III) oxidation in aqueous suspensions: reaction kinetics and effects of adsorption, Environ. Sci. Technol. 39 (2005) 1880–1886.
[34] P.K. Dutta, A.K. Ray, V.K. Sharma, F.J. Millero, Adsorption of arsenate and arsenite on titanium dioxide suspensions, J. Colloid Interface Sci. 278 (2004) 270–275.
[35] H. Jézéquel, K.H. Chu, Removal of arsenate from aqueous solution by adsorption onto titanium dioxide nanoparticles, J. Environ. Sci. Health, Part A 41 (2006) 1519–1528.
[36] H. Yang, W.Y. Lin, K. Rajeshwar, Homogeneous and heterogeneous photocatalytic reactions involving As(III) and As(V) species in aqueous media, J. Photochem. Photobiol. A 123 (1999) 137–143.
[37] H. Lee, W. Choi, Photocatalytic oxidation of arsenite in TiO_2 suspension: kinetics and mechanisms, Environ. Sci. Technol. 36 (2002) 3872–3878.
[38] P.M. Jayaweera, P.I. Godakumbura, K.A.S. Pathiratne, Photocatalytic oxidation of As(III) to As(V) in aqueous solutions: a low cost pre-oxidative treatment for total removal of arsenic from water, Curr. Sci. 84 (2003) 541–543.
[39] J. Ryu, W. Choi, Effects of TiO_2 surface modifications on photocatalytic oxidation of arsenite: the role of superoxides, Environ. Sci. Technol. 38 (2004) 2928–2933.
[40] P.K. Dutta, S.O. Pehkonen, V.K. Sharma, A.K. Ray, Photocatalytic oxidation of arsenic(III): evidence of hydroxyl radicals, Environ. Sci. Technol. 39 (2005) 1827–1834.
[41] M. Bissen, M.M. Vieillard-Baron, A.J. Schindelin, F.H. Frimmel, TiO_2-catalyzed photooxidation of arsenite to arsenate in aqueous samples, Chemosphere 44 (2001) 751–757.
[42] T.L. Xu, P.V. Kamat, K.E. O'Shea, Mechanistic evaluation of arsenite oxidation in TiO_2 assisted photocatalysis, J. Phys. Chem. A 109 (2005) 9070–9075.
[43] E.S. Tsimas, K. Tyrovola, N.P. Xekoukoulotakis, N.P. Nikolaidis, E. Diamadopoulos, D. Mantzavinos, Simultaneous photocatalytic oxidation of As(III) and humic acid in aqueous TiO_2 suspensions, J. Hazard. Mater. 169 (2009) 376–385.
[44] Z. Xu, X. Meng, Size effects of nanocrystalline TiO_2 on As(V) and As(III) adsorption and As(III) photooxidation, J. Hazard. Mater. 168 (2009) 747–752.
[45] H. Lin, C.P. Huang, W. Li, C. Ni, S.I. Shah, Y.-H. Tseng, Size dependency of nanocrystalline TiO_2 on its optical property and photocatalytic reactivity exemplified by 2-chlorophenol, Appl. Catal. B-Environ. 68 (2006) 1–11.
[46] S. Liu, N. Jaffrezic, C. Guillard, Size effects in liquid-phase photo-oxidation of phenol using nanometer-sized TiO_2 catalysts, Appl. Surf. Sci. 255 (2008) 2704–2709.
[47] M.N. Chong, B. Jin, C.W.K. Chow, C. Saint, Recent developments in photocatalytic water treatment technology: a review, Water Res. 44 (2010) 2997–3027.
[48] D.W. Chen, F.M. Li, A.K. Ray, External and internal mass transfer effect on photocatalytic degradation, Catal. Today 66 (2001) 475–485.
[49] S. Zheng, Y. Cai, K.E. O'Shea, TiO_2 photocatalytic degradation of phenylarsonic acid, J. Photochem. Photobiol. A 210 (2010) 61–68.
[50] C. Jing, X. Meng, E. Calvache, G. Jiang, Remediation of organic and inorganic arsenic contaminated groundwater using a nanocrystalline TiO_2-based adsorbent, Environ. Pollut. 157 (2009) 2514–2519.
[51] G. Jegadeesan, S.R. Al-Abed, V. Sundaram, H. Choi, K.G. Scheckel, D.D. Dionysiou, Arsenic sorption on TiO_2 nanoparticles: size and crystallinity effects, Water Res. 44 (2010) 965–973.

[52] H.Y. Niu, J.M. Wang, Y.L. Shi, Y.Q. Cai, F.S. Wei, Adsorption behavior of arsenic onto protonated titanate nanotubes prepared via hydrothermal method, Microporous Mesoporous Mater. 122 (2009) 28–35.
[53] M. Borho, P. Wilderer, Optimized removal of arsenate(III) by adaptation of oxidation and precipitation processes to the filtration step, Water Sci. Technol. 34 (1996) 25–31.
[54] M. Edwards, Chemistry of arsenic removal during coagulation and Fe—Mn oxidation, J. Am. Water Works Assoc. 86 (1994) 64–78.
[55] J.G. Hering, P.Y. Chen, J.A. Wilkie, M. Elimelech, S. Liang, Arsenic removal by ferric chloride, J. Am. Water Works Assoc. 88 (1996) 155–167.
[56] Z. Xu, Q. Li, S. Gao, J.K. Shang, As(III) removal by hydrous titanium dioxide prepared from one-step hydrolysis of aqueous $TiCl_4$ solution, Water Res. 44 (2010) 5713–5721.
[57] M. Pirilä, M. Martikainen, K. Ainassaari, T. Kuokkanen, R.L. Keiski, Removal of aqueous As(III) and As(V) by hydrous titanium dioxide, J. Colloid Interface Sci. 353 (2011) 257–262.
[58] S. Bang, M. Patel, L. Lippincott, X.G. Meng, Removal of arsenic from groundwater by granular titanium dioxide adsorbent, Chemosphere 60 (2005) 389–397.
[59] C. Gerente, V.K.C. Lee, P. Le Cloirec, G. McKay, Application of chitosan for the removal of metals from wastewaters by adsorption – mechanisms and models review, Crit. Rev. Environ. Sci. Technol. 37 (2007) 41–127.
[60] S.M. Miller, J.B. Zimmerman, Novel, bio-based, photoactive arsenic sorbent: TiO_2-impregnated chitosan bead, Water Res. 44 (2010) 5722–5729.
[61] S.M. Miller, M.L. Spaulding, J.B. Zimmerman, Optimization of capacity and kinetics for a novel bio-based arsenic sorbent, TiO_2-impregnated chitosan bead, Water Res. 45 (2011) 5745–5754.
[62] J. Qu, Research progress of novel adsorption processes in water purification: a review, J. Environ. Sci.-China 20 (2008) 1–13.
[63] S. Yao, Y. Jia, Z. Shi, S. Zhao, Photocatalytic oxidation of arsenite by a composite of titanium dioxide and activated carbon fiber, Photochem. Photobiol. 86 (2010) 1215–1221.
[64] T.V. Nguyen, S. Vigneswaran, H.H. Ngo, J. Kandasamy, H.C. Choi, Arsenic removal by photo-catalysis hybrid system, Sep. Purif. Technol. 61 (2008) 44–50.
[65] T. Nakajima, Y.H. Xu, Y. Mori, M. Kishita, H. Takanashi, S. Maeda, A. Ohki, Combined use of photocatalyst and adsorbent for the removal of inorganic arsenic(III) and organoarsenic compounds from aqueous media, J. Hazard. Mater. 120 (2005) 75–80.
[66] S.H. Yoon, J.H. Lee, Combined use of photochemical reaction and activated alumina for the oxidation and removal of arsenic(III), J. Ind. Eng. Chem. 13 (2007) 97–104.
[67] A.H. Fostier, M.d.S. Silva Pereira, S. Rath, J.R. Guimaraes, Arsenic removal from water employing heterogeneous photocatalysis with TiO_2 immobilized in PET bottles, Chemosphere 72 (2008) 319–324.
[68] G.-S. Zhang, J.-H. Qu, H.-J. Liu, R.-P. Liu, G.-T. Li, Removal mechanism of As(III) by a novel Fe—Mn binary oxide adsorbent: oxidation and sorption, Environ. Sci. Technol. 41 (2007) 4613–4619.
[69] X. Dou, Y. Zhang, M. Yang, Y. Pei, X. Huang, T. Takayama, S. Kato, Occurrence of arsenic in groundwater in the suburbs of Beijing and its removal using an iron—cerium bimetal oxide adsorbent, Water Qual. Res. J. Can. 41 (2006) 140–146.
[70] K. Gupta, T. Basu, U.C. Ghosh, Sorption characteristics of arsenic(V) for removal from water using agglomerated nanostructure iron(III)—zirconium(IV) bimetal mixed oxide, J. Chem. Eng. Data 54 (2009) 2222–2228.
[71] Y. Zhang, M. Yang, X.M. Dou, H. He, D.S. Wang, Arsenate adsorption on an Fe—Ce bimetal oxide adsorbent: role of surface properties, Environ. Sci. Technol. 39 (2005) 7246–7253.
[72] Y. Zhang, M. Yang, H. He, X. Huang, Characterization of a bimetal oxide adsorbent and its adsorption mechanism for arsenic(V), Abstr. Pap. Am. Chem. Soc. 226 (2003) U597.
[73] G. Zhang, J. Qu, H. Liu, R. Liu, R. Wu, Preparation and evaluation of a novel Fe—Mn binary oxide adsorbent for effective arsenite removal, Water Res. 41 (2007) 1921–1928.
[74] S. Deng, Z. Li, J. Huang, G. Yu, Preparation, characterization and application of a Ce—Ti oxide adsorbent for enhanced removal of arsenate from water, J. Hazard. Mater. 179 (2010) 1014–1021.
[75] Z. Li, S. Deng, G. Yu, J. Huang, V.C. Lim, As(V), As(III) removal from water by a Ce—Ti oxide adsorbent: behavior and mechanism, Chem. Eng. J. 161 (2010) 106–113.
[76] K. Gupta, U.C. Ghosh, Arsenic removal using hydrous nanostructure iron(III)—titanium(IV) binary mixed oxide from aqueous solution, J. Hazard. Mater. 161 (2009) 884–892.
[77] B. Manna, M. Dasgupta, U.C. Ghosh, Crystalline hydrous titanium (IV) oxide (CHTO): an arsenic (III) scavenger from natural water, J. Water Supply Res. Technol. 53 (2004) 483–495.
[78] M. D'Arcy, D. Weiss, M. Bluck, R. Vilar, Adsorption kinetics, capacity and mechanism of arsenate and phosphate on a bifunctional TiO_2—Fe_2O_3 bi-composite, J. Colloid Interface Sci. 364 (2011) 205–212.
[79] F.-S. Zhang, H. Itoh, Photocatalytic oxidation and removal of arsenite from water using slag-iron oxide-TiO_2 adsorbent, Chemosphere 65 (2006) 125–131.
[80] W. Zhou, H. Fu, K. Pan, C. Tian, Y. Qu, P. Lu, C.-C. Sun, Mesoporous TiO_2/alpha-Fe_2O_3. Bifunctional composites for effective elimination of arsenite contamination through simultaneous photocatalytic oxidation and adsorption, J. Phys. Chem. C 112 (2008) 19584–19589.
[81] H. Jezequel, K.H. Chu, Enhanced adsorption of arsenate on titanium dioxide using Ca and Mg ions, Environ. Chem. Lett. 3 (2005) 132–135.
[82] Z.H. Xu, X.G. Meng, Size effects of nanocrystalline TiO_2 on As(V) and As(III) adsorption and As(III) photooxidation, J. Hazard. Mater. 168 (2009) 747–752.
[83] C.H. Swartz, N.K. Blute, B. Badruzzman, A. Ali, D. Brabander, J. Jay, J. Besancon, S. Islam, H.F. Hemond, C.F. Harvey, Mobility of arsenic in a Bangladesh aquifer: inferences from geochemical profiles, leaching data, and mineralogical characterization, Geochim. Cosmochim. Acta 68 (2004) 4539–4557.
[84] J. Ma, N.J.D. Graham, Degradation of atrazine by manganese-catalysed ozonation – influence of radical scavengers, Water Res. 34 (2000) 3822–3828.
[85] G. Liu, X. Zhang, J.W. Talley, C.R. Neal, H. Wang, Effect of NOM on arsenic adsorption by TiO_2 in simulated As(III)-contaminated raw waters, Water Res. 42 (2008) 2309–2319.
[86] G.J. Liu, X.R. Zhang, L. Mcwilliams, J.W. Talley, C.R. Neal, Influence of ionic strength, electrolyte type, and NOM on As(V) adsorption onto TiO_2, J. Environ. Sci. Health A 43 (2008) 430–436.
[87] S.H. Yoon, J.H. Lee, Oxidation mechanism of As(III) in the UV/TiO_2 system: evidence for a direct hole oxidation mechanism, Environ. Sci. Technol. 39 (2005) 9695–9701.
[88] V.K. Sharma, P.K. Dutta, A.K. Ray, Review of kinetics of chemical and photocatalytical oxidation of arsenic(III) as influenced by pH, J. Environ. Sci. Health A 42 (2007) 997–1004.
[89] B.H.J.B. Ulrik, K. Klaening, K. Sehested, Arsenic(I.V)., A pulse-radiolysis study, Inorg. Chem. 28 (1989) 2717–2724.
[90] J. Ryu, W.Y. Choi, Photocatalytic oxidation of arsenite on TiO_2: understanding the controversial oxidation mechanism involving superoxides and the effect of alternative electron acceptors, Environ. Sci. Technol. 40 (2006) 7034–7039.
[91] S.-H. Yoon, S.-E. Oh, J.E. Yang, J.H. Lee, M. Lee, S. Yu, D. Pak, TiO_2 photocatalytic oxidation mechanism of As(III), Environ. Sci. Technol. 43 (2009) 864–869.
[92] H. Fei, W.H. Leng, X. Li, X.F. Cheng, Y.M. Xu, J.Q. Zhang, C.N. Caom, Photocatalytic oxidation of arsenite over TiO_2: is superoxide the main oxidant in normal air-saturated aqueous solutions? Environ. Sci. Technol. 45 (2011) 4532–4539.
[93] M. Pena, X.G. Meng, G.P. Korfiatis, C.Y. Jing, Adsorption mechanism of arsenic on nanocrystalline titanium dioxide, Environ. Sci. Technol. 40 (2006) 1257–1262.
[94] G. Jegadeesan, V. Sundaram, H. Choi, D. Dionysiou, S.R. Al-Abed, Arsenic removal using titanium dioxide nanoparticles synthesized with sol–gel methods, Abstr. Pap. Am. Chem. Soc. 232 (2006) 627-627.
[95] C.Y. Jing, X.G. Meng, S.Q. Liu, S. Baidas, R. Patraju, C. Christodoulatos, G.P. Korfiatis, Surface complexation of organic arsenic on nanocrystalline titanium oxide, J. Colloid Interface Sci. 290 (2005) 14–21.
[96] T.L. Xu, Y. Cai, K.E. O'Shea, Adsorption and photocatalyzed oxidation of methylated arsenic species in TiO_2 suspensions, Environ. Sci. Technol. 41 (2007) 5471–5477.